

Supplemental Information

Coactivator-dependent metabolic reprogramming is a survival strategy required for prostate tumor metastasis

Subhamoy Dasgupta, Nagireddy Putluri, Weiwen Long, Bin Zhang, Jianghua Wang, Akash K. Kaushik, James M. Arnold, Salil K. Bhowmik, Erin Stashi, Christine A. Brennan, Kimal Rajapakshe, Cristian Coarfa, Nicholas Mitsiades, Michael M. Ittmann, Arul M. Chinnaiyan, Arun Sreekumar, Bert W. O'Malley

List of Supplemental Material Page

1. Supplemental Figures

Figure S1, related to Figure 1

Figure S2, related to Figure 2

Figure S3, related to Figure 2

Figure S4, related to Figure 2

Figure S5, related to Figure 3

Figure S6, related to Figure 4

Figure S7, related to Figure 5

Figure S8, related to Figure 5

Figure S9, related to Figure 6

Figure S10, related to Figure 7

Figure S11, related to Figure 8

Figure S12, related to Figure 8

Figure S13, related to Figure 9

2. Supplemental Figure Legends

Supplemental Figures S1-S13.

3. Supplemental Tables

Table S1, related to Figure 2.

4. Supplemental Experimental Procedures

5. Supplemental References

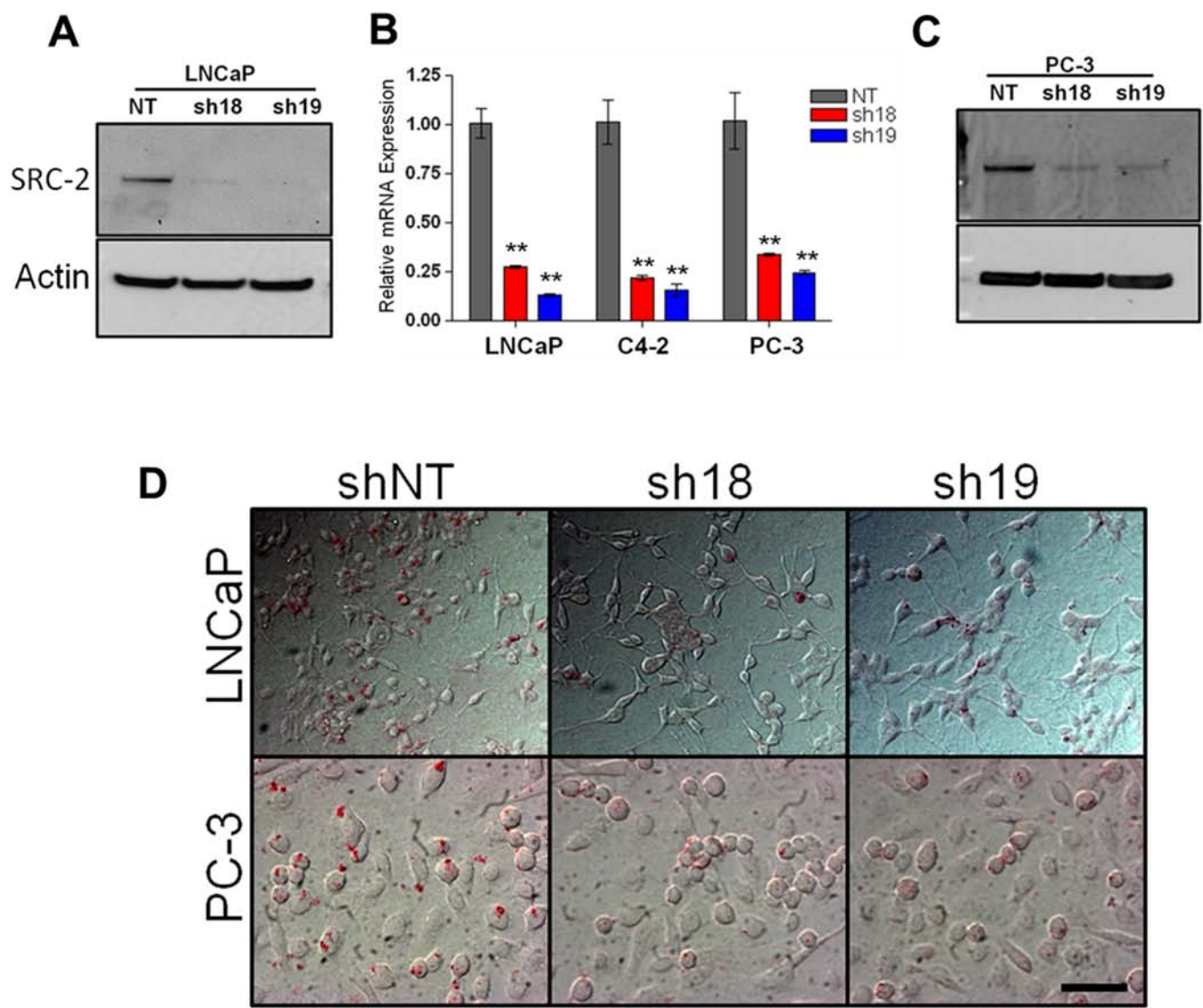


Figure. S1

Figure S1. SRC-2 ablated prostate cancer cells show reduced lipid droplet formation.

(A, C) Western blot analysis showing the expression of SRC-2 and actin in LNCaP and PC-3 cells stably expressing non-targeting shRNA (shNT), and two different clones of SRC-2 shRNA (sh18 and sh19). Actin was used to normalize the protein loading.

(B) Quantitative real time PCR analysis of SRC-2 gene expression in LNCaP and PC-3 stable cells- shNT, sh18 and sh19 ($n=4$). Data are graphed as the mean \pm s.e.m. $**P<0.001$ by Student's *t* test.

(D) Oil Red-O staining of LNCaP and PC-3 stable cells- shNT, sh18 and sh19. Scale bar 10 μ m.

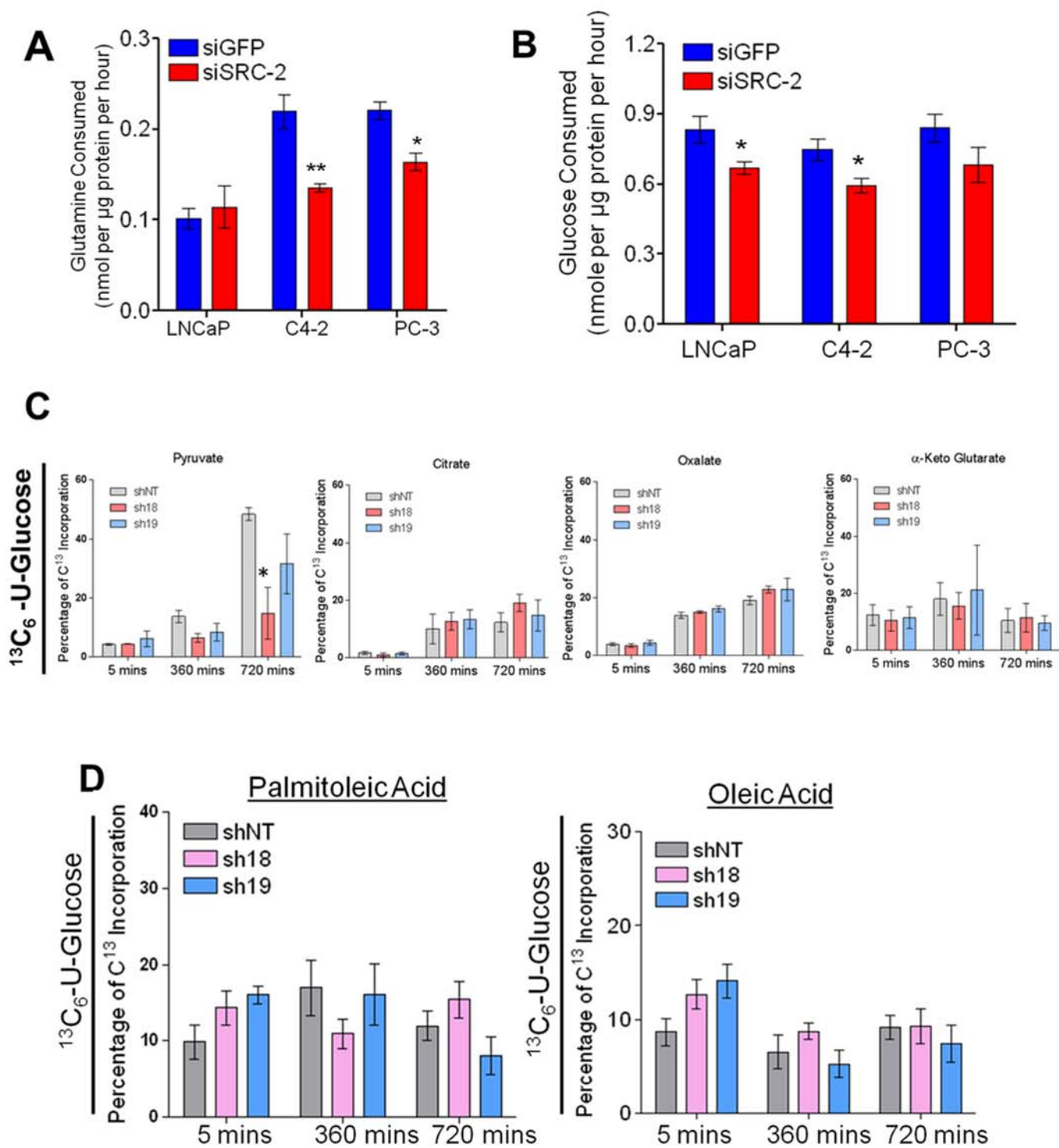


Figure. S2

Figure S2. Glucose and glutamine consumption in prostate cancer cells, and mass isotopomeric analysis showing incorporation of [U-13C]glucose carbons in TCA metabolites.

(A, B) Relative consumption of glucose and glutamine in LNCaP, C4-2 and PC-3 cells treated with control-siRNA (siGFP) or SRC-2-siRNA (siSRC-2) ($n=5/\text{group}$).

(C) C4-2 stable cells- shNT, sh18 and sh19 were cultured in presence of D[U-¹³C₆]glucose for indicated time followed by mass isotopomer analysis. Graphical representation shows the percentage incorporation of D[U-¹³C₆]glucose -derived C¹³ in citrate, α -keto glutarate, oxalate and pyruvate ($n=3/\text{group}$).

(D) Graphical representation shows the percentage incorporation of D[U-¹³C₆]glucose -derived C¹³ in palmitoleic and oleic acid at different time points.

Data are graphed as the mean \pm s.e.m. * $P<0.05$, ** $P<0.001$ by 2-way Anova with Tukey's multiple comparison test.

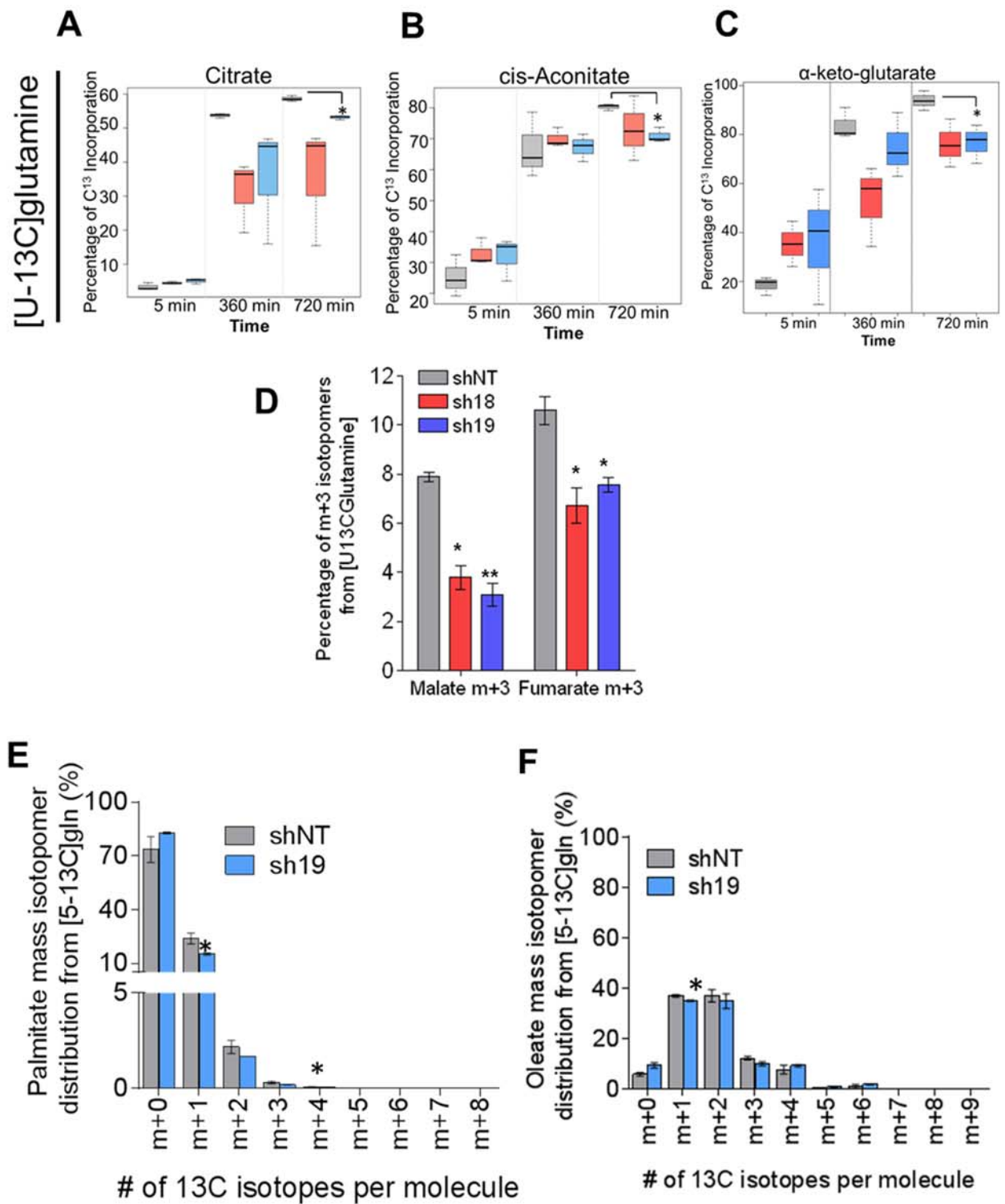


Figure. S3

Figure S3. SRC-2 promotes reductive carboxylation of glutamine for fatty acid biosynthesis.

(A-C) Metabolites were extracted at indicated time-points from C4-2 stable cells- shNT, sh18 and sh19 cultured in presence of 2mM- L-[U-¹³C₅]glutamine and 11mM of unlabelled glucose after addition of tracers. Mass isotopomer analysis demonstrating the total percentage of glutamine-C¹³ incorporated in citrate, cis-aconitate, and α-ketoglutarate (*n*=3/group). The boxplot shows the 5% and 95% quantiles (whiskers), 25% and 75% quartiles (box), and the median marked by horizontal line. **q*<0.05, ***q*<0.001 by two-sided *t* test with a FDR-corrected *P*<0.05 was considered significant.

(D) Relative levels of malate *m*+3 and fumarate *m*+3 isotopomer with from -[U-13C]glutamine. **P*<0.05, ***P*<0.001 by 2-way Anova with Tukey's multiple comparison test.

(E, F) Mass isotopomer distribution of palmitate and oleate extracted from C4-2 stable cells- shNT (non-targeting), shSRC-2- sh19 cultured in presence of 2mM [5-13C]glutamine and 11mM unlabelled glucose (*n*=3/group). **P*<0.05, by Student's *t* test with Holm-Sidak's multiple comparison test.

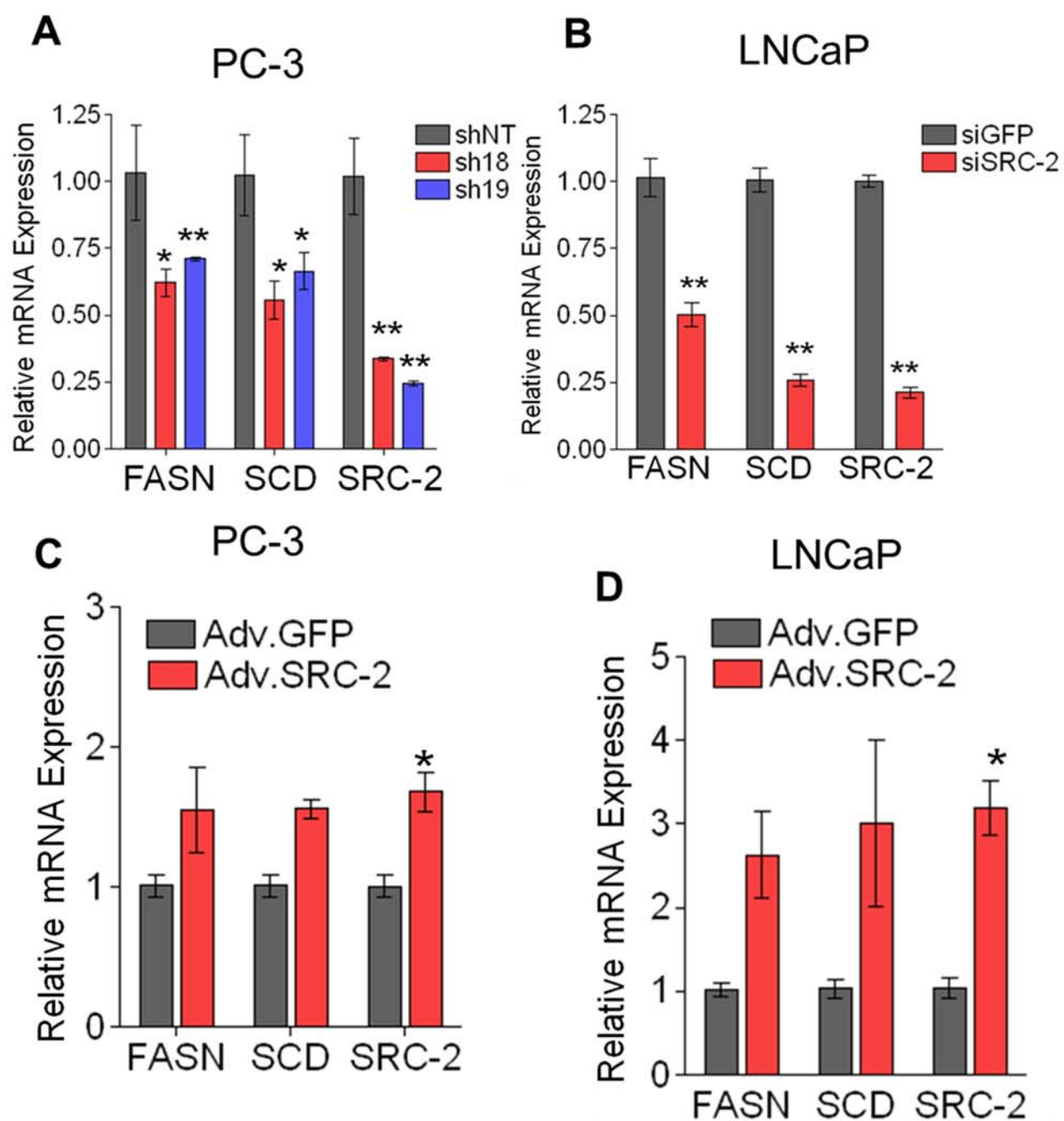


Figure. S4

Figure S4. SRC-2 modulates FASN and SCD expression.

Quantitative real time PCR analysis of FASN, SCD, and SRC-2 gene expression relative to actin.

(A) PC-3 stable cells expressing shNT, sh18, and sh19.

(B) LNCaP cells treated with control siRNA (siGFP) or SRC-2-siRNA (siSRC-2),

(C) PC-3 cells expressing control adenovirus (Adv.GFP) or SRC-2 adenovirus (Adv.SRC-2),

(D) LNCaP cells expressing control adenovirus (Adv.GFP) or SRC-2 adenovirus (Adv.SRC-2).

Data are graphed as the mean \pm s.e.m. * P <0.05, ** P <0.001 by Student's t test.

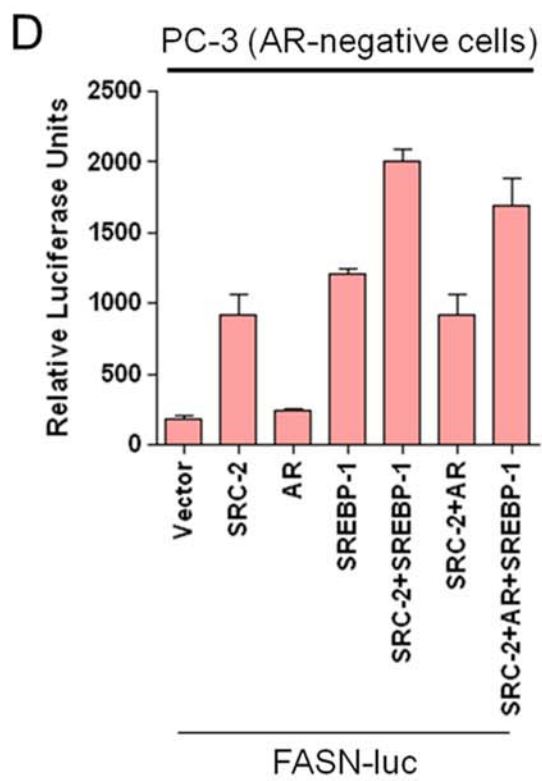
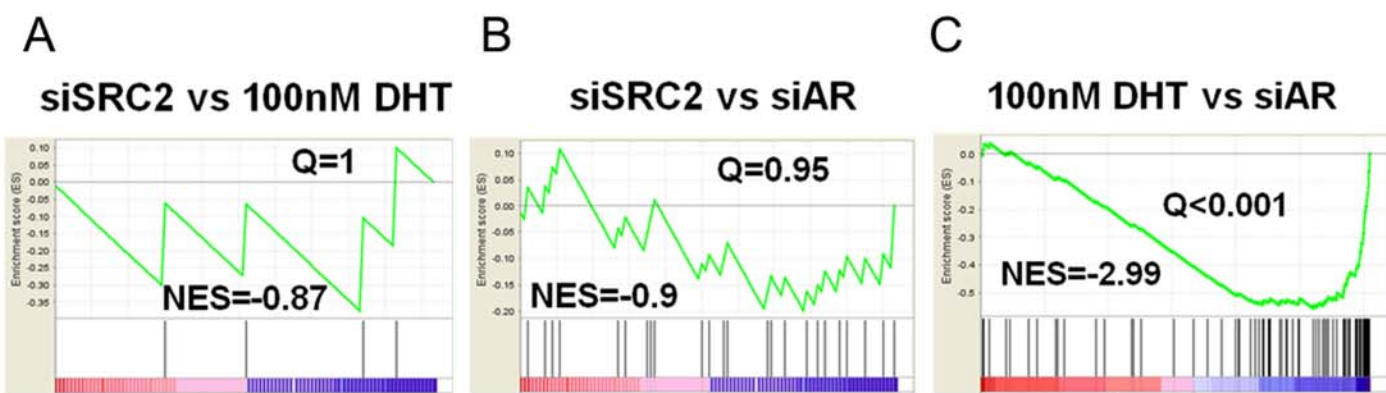


Figure. S5

Figure S5. SRC-2 transcriptionally regulates fatty acid biosynthetic genes independent of AR. Comparison of gene set enrichment analysis (GSEA) of siSRC-2 and siAR gene signatures with androgen (100nM of dihydroxytestosterone) responsive signatures.

(A) siSRC2 vs 100nM DHT, 24hrs, NES=, $q=1$;

(B) siSRC-2 vs siAR, NES=-0.9, $q=0.95$;

(C) siAR vs 100 nM DHT, 24hrs, NES=-2.99, $Q<0.001$.

(D) Luciferase reporter assay in PC-3 cells transiently transfected with FASN-luciferase construct along with empty vector (pcDNA3.1), SRC-2, AR, SREBP-1a, or in combination. Luciferase values normalized to protein level ($n=6$ /group). Data are graphed as the mean \pm s.e.m. * $P<0.05$, by Student's t test. Data are presented as relative fold expression normalized to actin.

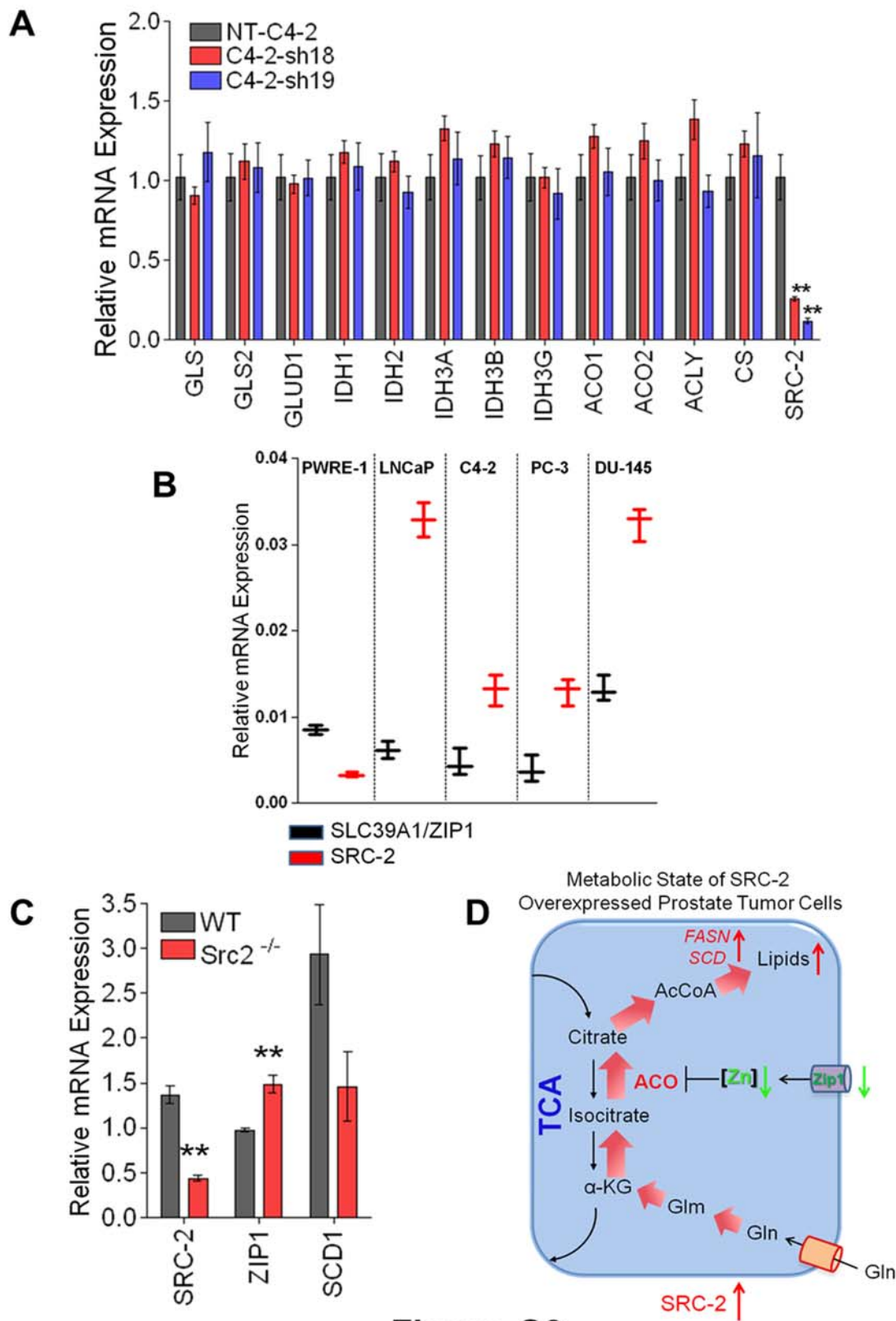


Figure. S6

Figure S6. SRC-2 represses ZIP1 (SLC39A1) expression to induce activation of aconitase enzyme.

(A) Quantitative real time PCR analysis of *GLS*, *GLS1*, *GLUD1*, *IDH1*, *IDH2*, *IDH3B*, *IDH3G*, *ACO1*, *ACO2*, *ACLY*, *CS* and *SRC-2* gene expression in C4-2 stable cells- shNT, sh18 and sh19. ** $P < 0.001$ by Student's *t* test.

(B) Quantitative real time PCR analysis of SRC-2 and ZIP1 expression in transformed normal prostate epithelial cell line PWRE-1, and tumor lines LNCaP, C4-2, PC-3 and DU-145. Data are presented as relative fold expression normalized to actin. Data are graphed as the mean \pm s.e.m.

(C) Quantitative real time PCR analysis of *Src-2*, *Zip1(Slc39a1)*, and *Scd1* from wildtype (WT) and SRC-2 knockout (*Src-2^{-/-}*) mouse prostate ($n=8$). SCD1 was used as a control. ** $P < 0.001$, by 2-way Anova with Tukey's multiple comparison test.

(D) Cartoon depicting the proposed metabolic state of SRC-2 overexpressed prostate tumor cells. SRC-2 promotes glutamine (Gln) anaplerotic pathway by inducing reductive carboxylation of α -ketoglutarate (α KG) to generate citrate. This is facilitated by SRC-2 dependent repression of SLC39A1 (ZIP1), a Zn transporter thereby stimulating aconitase (ACO) enzymatic activity. Citrate is then converted into acetyl-CoA and eventually used for *de novo* lipogenesis by SRC-2 target enzymes FASN and SCD, thus promoting lipogenesis in prostate tumor cells.

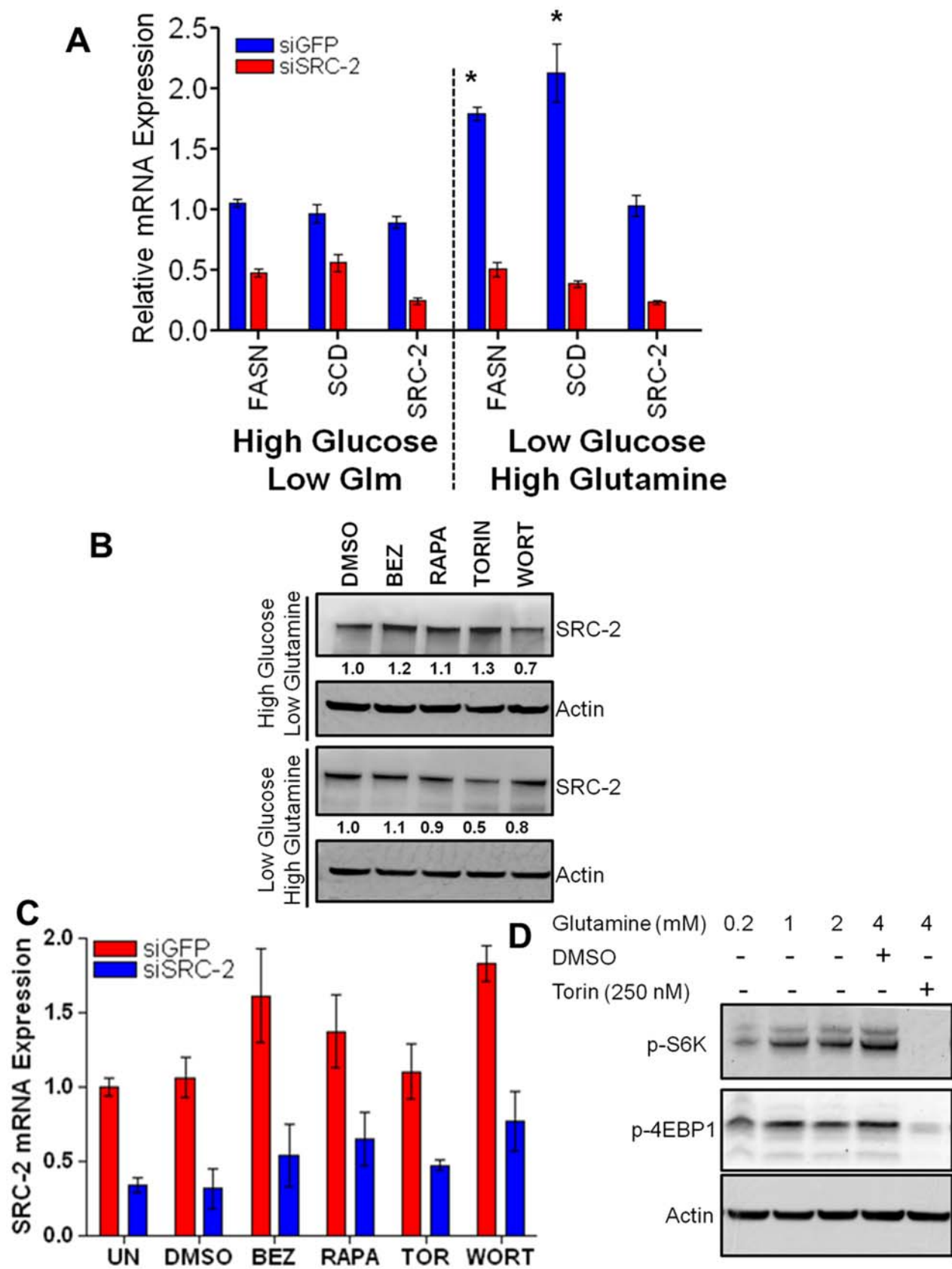


Figure. S7

Figure S7. Glutamine stimulation activates SRC-2 transcriptional functions in an mTORC1 dependent manner.

(A) Quantitative real time PCR analysis of FASN, SCD and SRC-2 in C4-2 cells were treated with siGFP (control) or siSRC-2 and cultured in nutrient stressed conditions- high glucose (11mM)/low glutamine (0.2mM) or low glucose (5mM)/high glutamine (2mM) ($n=3$ /group). * $P<0.05$, by Student's t test.

(B) C4-2 cells were cultured in presence of high glucose (11mM)/low glutamine (0.2mM) or low glucose (5mM)/high glutamine (2mM) and then treated with kinase inhibitors: BEZ-235 (1 μ M); Rapamycin (100nM); Torin (250nM); and Wortmannin (250nM). Western blot analyses were performed to measure the stability of SRC-2 protein. Semi-quantitative levels of each band were analyzed by densitometry using UVP Vision Works LS software and relative values (compared to DMSO) normalized to actin are indicated numerically under each lane.

(C) Quantitative real time PCR analysis of SRC-2 in C4-2 cells expressing siGFP (control) or siSRC-2 and then treated with BEZ-235 (1 μ M); Rapamycin (100nM); Torin (250nM); and Wortmannin (250nM) ($n=3$ /group).

(D) Western blot analysis showing the expression of phospho-S6K (p-S6K), phospho-4EBP1 (p-4EBP1) and actin in C4-2 cells stimulated with increasing concentration of glutamine followed by treatment with DMSO or mTORC1 inhibitor-Torin. Actin was used to normalize the protein loading. Data are presented as relative fold expression normalized to actin.

Data are graphed as the mean \pm s.e.m.

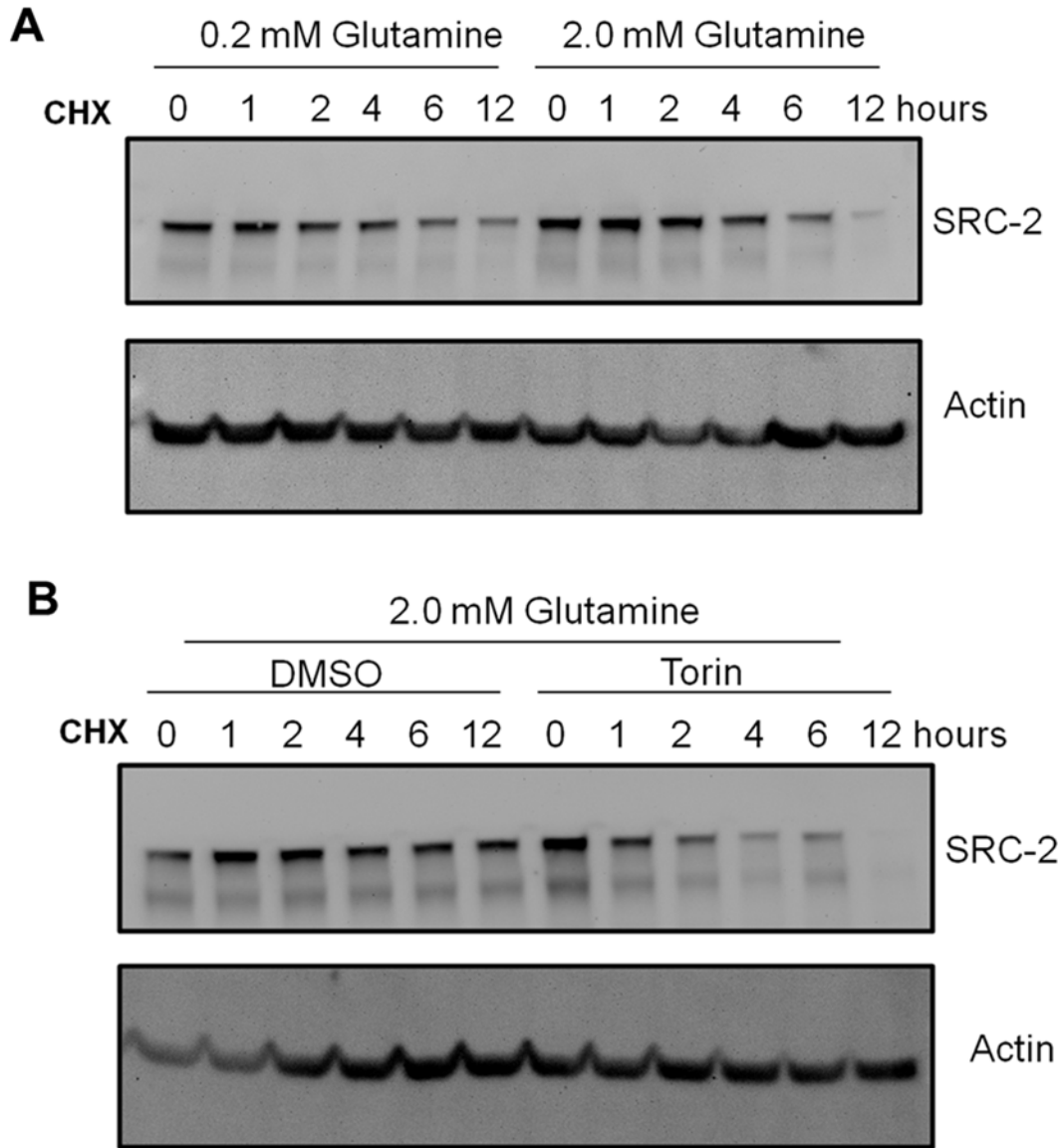


Figure. S8

Figure S8. Glutamine-dependent mTORC1 phosphorylation controls SRC-2 protein stability.

(A) C4-2 cells were cultured in presence of low glutamine (0.2mM) and high glutamine (2.0mM) followed by treatment with cycloheximide (0.5mM) for indicated time points. Western blot showing the total-level of SRC-2 and actin was used as a loading control.

(B) C4-2 cells were cultured in presence of high glutamine (2.0mM) followed by either treatment with DMSO and Torin. Cycloheximide (0.5mM) was then added to the cells for indicated time points. Western blot showing the total-level of SRC-2 and actin was used as a loading control.

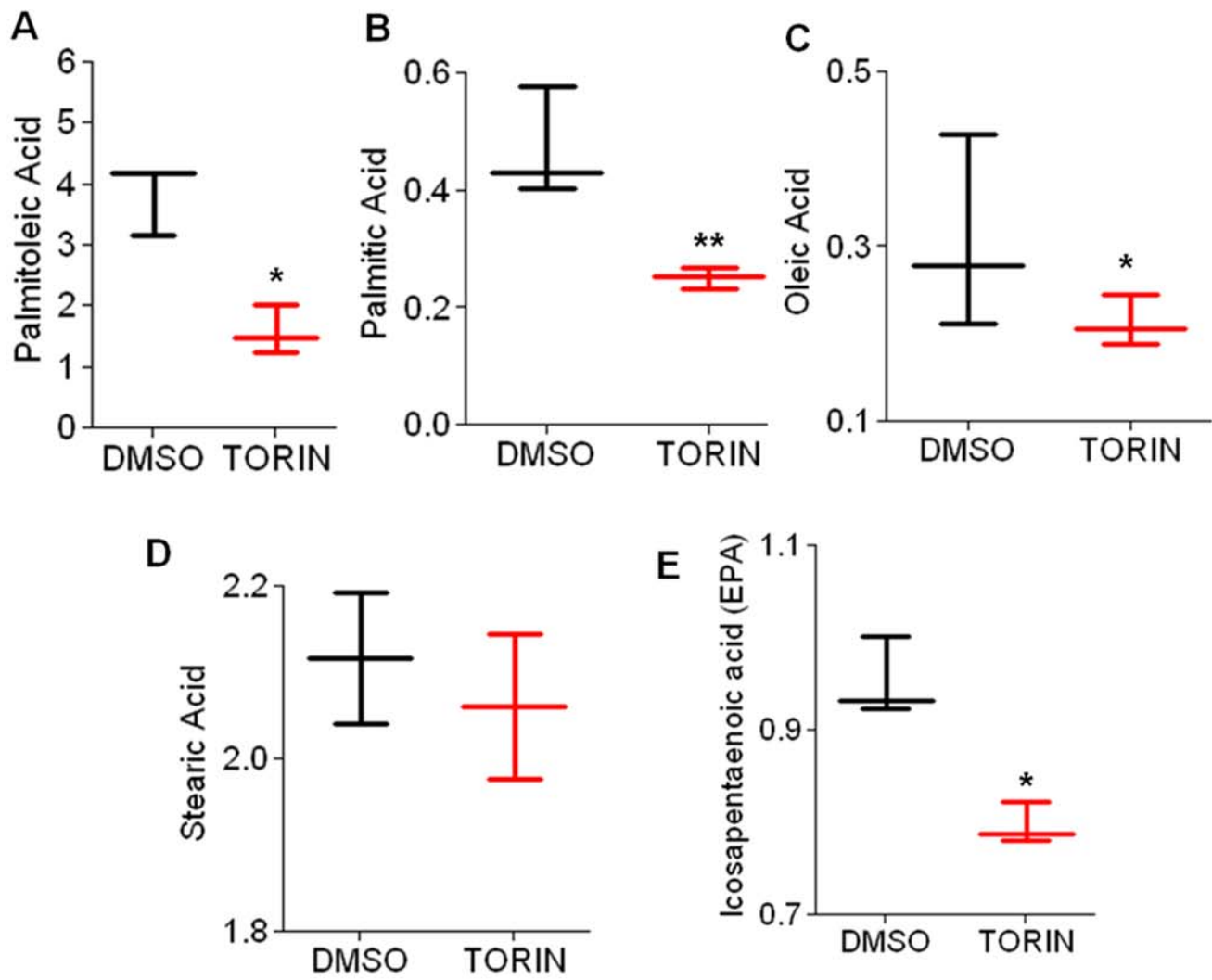


Figure. S9

Figure S9. mTORC1-inhibitor Torin decreases lipid levels in C4-2 prostate cancer cell line.

(A-E) Targeted mass spectrometry based-metabolomics analyses demonstrating the relative levels of palmitoleic, palmitic, oleic, stearic and icosapentaenoic acid (EPA) in C4-2 cells treated with Torin or DMSO control ($n=3$ /group). Data are presented as relative fold expression as a Box and whiskers plot showing the minimum to maximum (whiskers), 25% and 75% quartiles (box), and the median marked by horizontal line. * $P<0.05$, ** $P<0.001$ considered significant by two-tailed paired t test.

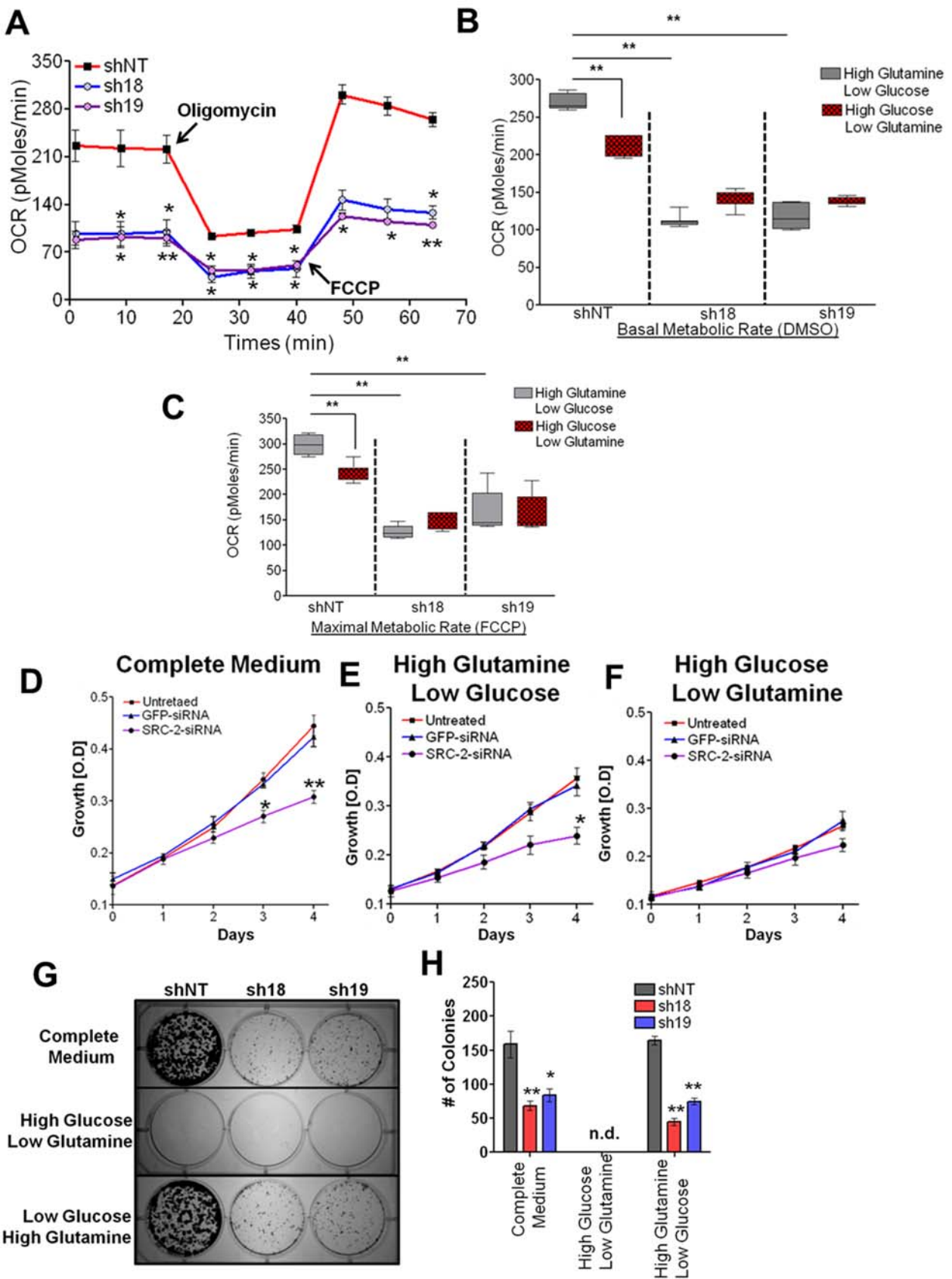


Figure. S10

Figure S10. Depletion of SRC-2 represents a metabolically deficient phenotype.

(A) Real-time measurement of basal and maximal oxygen consumption rate (OCR) in PC-3 stable cells- shNT, sh18, and sh19 ($n=3/\text{group}$). $*P<0.05$, $**P<0.001$ vs shNT, by 2-way Anova with Tukey's multiple comparison test.

(B, C) Basal and maximal OCR in PC-3 stable cells- shNT, sh18, and sh19 were measured in DMSO control or FCCP-treated cells cultured in presence of high glucose (11mM)/low glutamine (0.2mM) or low glucose (5mM)/high glutamine (2mM). Box and whiskers plot were prepared showing the minimum to maximum (whiskers), 25% and 75% quartiles (box), and the median marked by horizontal line. $*P<0.05$, $**P<0.001$ by Two-tailed t test.

(D-F) Growth curve of C4-2 cells treated with control GFP-siRNA or SRC-2-siRNA, and cultured in complete medium (11mM glucose and 2mM glutamine); high glucose (11mM)/low glutamine (0.2mM); or low glucose (5mM)/high glutamine (2mM) for 4 days. $*P<0.05$, $**P<0.001$ vs shNT, by 2-way Anova with Tukey's multiple comparison test.

(G) Clonogenic survival assay showing the number of C4-2 stable cell- shNT, sh18, and sh19 clones that survived after 2 weeks of nutrient stress.

(H) Graphical representation of the number of colonies shown in (G). n.d: not determined. Data are graphed as the mean \pm s.e.m. $*P<0.05$, $**P<0.001$ by Student's t test.

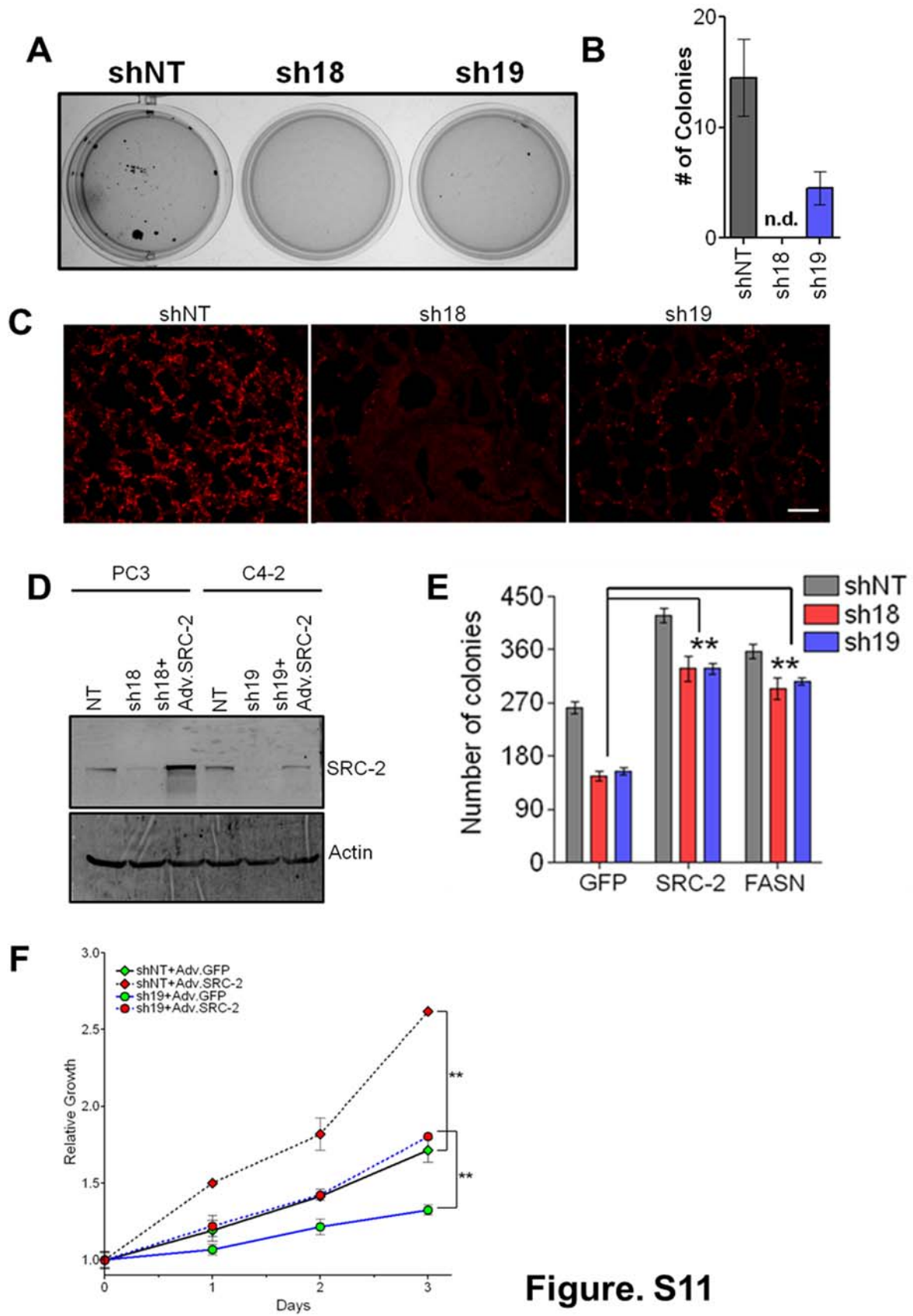


Figure. S11

Figure S11. Depletion of SRC-2 impairs prostate cancer cell survival.

(A) Anchorage independent growth of PC-3 stable cells- shNT, sh18, and sh19 in soft agar assay two weeks after plating.

(B) Graphical representation of the number of stained colonies in PC-3 stable cells- shNT, sh18, and sh19. N.D. stands for not determined. Data are graphed as the mean \pm s.e.m. * P <0.05, ** P <0.001 by Student's t test.

(C) Representative images of Ki67 stained mouse lungs sections from PC-3-shNT, sh18 and sh19-injected animals. Scale bar: 100 μ m.

(D) Western blot analysis showing the expression of SRC-2 and actin in PC-3 stable cells- shNT, sh18, and sh18 infected with Adv. SRC-2; and C4-2 stable cells- shNT, sh19 and sh19 infected with Adv. SRC-2. Actin was used to normalize the protein loading.

(E) Graphical representation of the number of colonies shown in Figure 8F. Data are graphed as the mean \pm s.e.m. * P <0.05, ** P <0.001 by Student's t test.

(F) Growth curve of C4-2 stable cells- shNT and sh19 infected with either Adv. GFP or Adv. SRC-2 ($n=6$ /group). ** P <0.001 by 2-way Anova with Tukey's multiple comparison test.

Data are graphed as the mean \pm s.e.m. * P <0.05, ** P <0.001 by Student's t test. Scale bar 10 μ m.

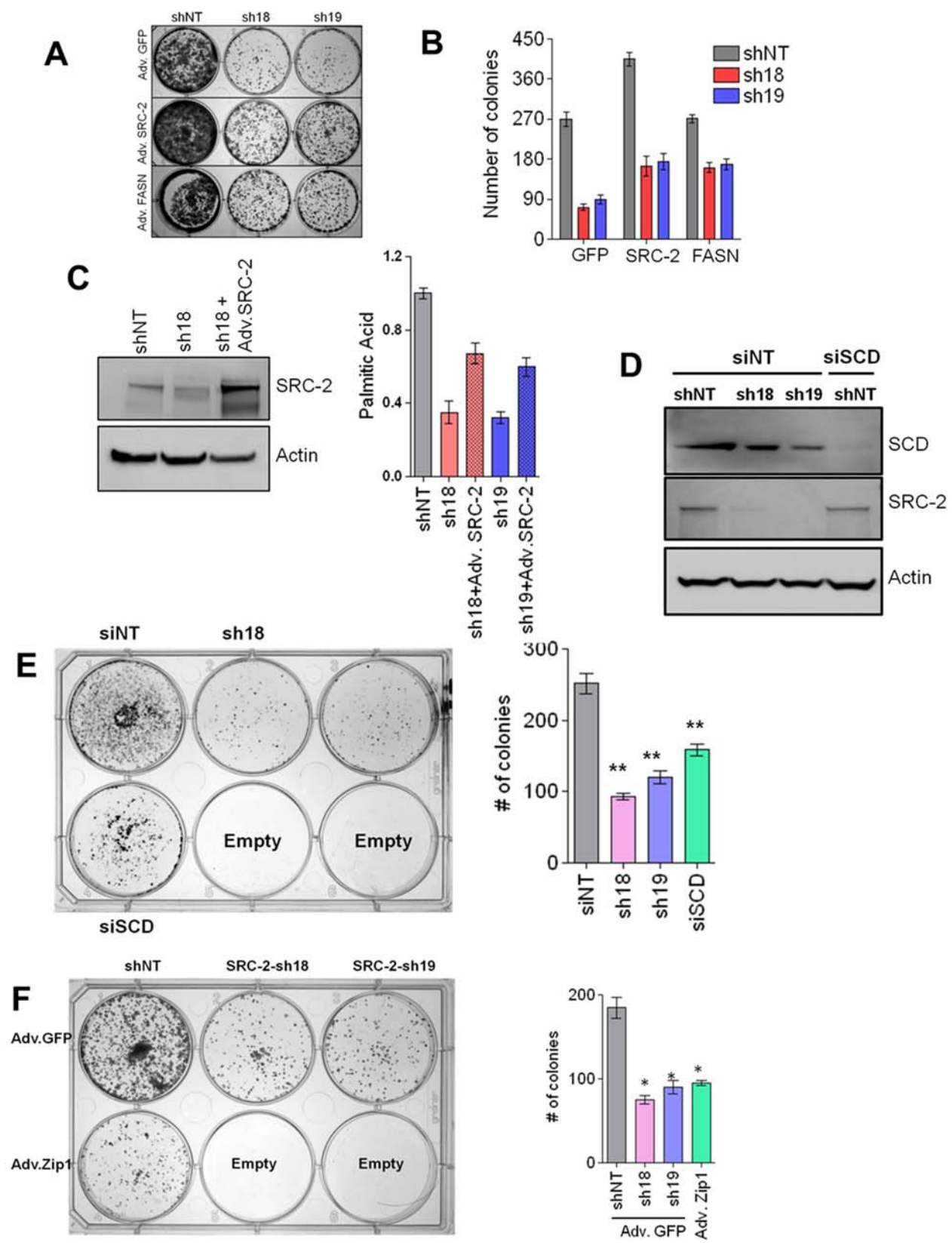


Figure. S12

Figure S12. Growth-defective phenotypes due to loss of SRC-2 could be rescue by SRC-2 downstream target genes.

(A) Clonogenic survival assay in PC-3 stable cells expressing Adv.GFP, Adv.SRC-2 or Adv.FASN to rescue the defective survival phenotype in SRC-2-depleted cells.

(B) Graphical representation of the number of colonies shown in (A).

(C) Western blot demonstrating the rescue of SRC-2 expression using Adv. SRC-2, followed by targeted mass spectrometry based-metabolomics analyses demonstrating the relative levels of palmitic acid.

(D) Western blot analysis showing the effect of siRNA targeting SCD in C4-2 stable cells.

(E) Clonogenic survival assay in C4-2 stable cells- shNT, sh18, and sh19 treated with siRNA-non-targeting (siNT) or siRNA-SCD. Graphical representation of the number of colonies

(F) Clonogenic survival assay in C4-2 stable cells expressing Adv.GFP, or Adv.Zip1. Graphical representation of the total number of colonies.

Data are graphed as the mean \pm s.e.m. * P <0.05, ** P <0.001 by Student's t test.

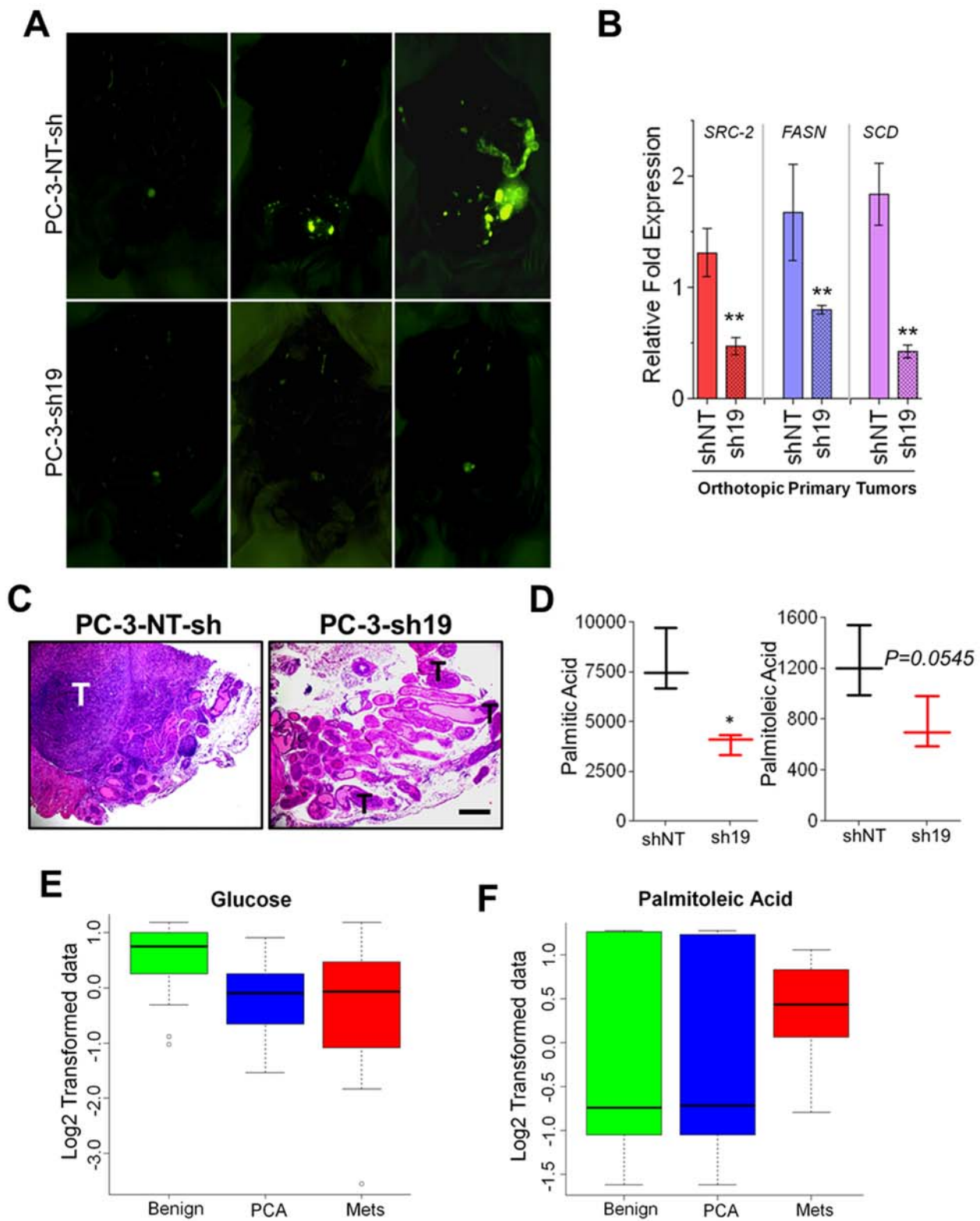


Figure. S13

Figure S13. Rescue by overexpression of SRC-2 or FASN restores survival deficiency of SRC-2-depleted prostate cancer cells.

(A) GFP-fluorescence images (excitation: 480nm, and emission: 510nm) showing the primary tumor and metastatic spread in *SCID* mouse injected with PC-3 stable cells- shNT and sh19 orthotopically in mouse prostate ($n=5$ /group) (merged images shown in Figure 9A).

(B) Quantitative real time PCR analysis of FASN, SCD and SRC-2 in PC-3 orthotopic primary prostate tumors expressing non-targeting shRNA (sh-NT) or SRC-2-shRNA-19 (sh19). Data are graphed as the mean \pm s.e.m. $**P<0.001$ by Student's *t* test.

(C) H&E stained sections of PC-3 orthotopic primary prostate tumors expressing non-targeting shRNA (sh-NT) or SRC-2-shRNA-19 (sh19). T- indicates the tumor area. Scale 100um.

(D) Targeted mass spectrometric analysis of xenograft-tumor extracts from PC-3-shNT and sh19 depicted in (A) showing the relative palmitic and palmitoleic acid levels ($n=5$ /group).

(E, F) Log₂ Transformed data depicting the levels of glucose and palmitoleic acid in cohort of prostate tissues from benign adjacent prostate ($n = 16$), clinically localized prostate cancer ($n = 12$, PCA) and metastatic prostate cancer ($n = 14$), as reported before by (1). For metabolomic analyses we performed a permutation based *P*-value (10000 permutation of sample labels) to define the significance of metabolites in different categories. The data was plotted as a boxplot in R language, showing the 5% and 95% quantiles (whiskers), 25% and 75% quartiles (box), and the median marked by horizontal line. $*q<0.05$, $**q<0.001$ by two-sided *t* test with a FDR-corrected $P<0.05$ was considered significant.

Table: S1

		Fold Change (comparing to siGFP-Control)			
		siRNA-SRC-2			
		Fold Change	95% CI	Comments	Fold Regulation
A01	SRC1	1.2544	(1.16, 1.34)	OKAY	1.2544
A02	SRC2	0.2331	(0.21, 0.25)	OKAY	-4.2894
A03	SRC3	1.3666	(1.25, 1.48)	OKAY	1.3666
A04	CS	1.2065	(1.09, 1.33)	OKAY	1.2065
A05	IDH1	0.8113	(0.74, 0.88)	OKAY	-1.2325
A06	ACTB	0.9251	(0.85, 1.00)	OKAY	-1.0809
A07	GAPDH	0.9344	(0.84, 1.02)	OKAY	-1.0702
A08	IDH2	0.8208	(0.75, 0.89)	OKAY	-1.2183
A09	IDH3A	1.2761	(1.19, 1.36)	OKAY	1.2761
A10	IDH3B	1.2227	(1.13, 1.32)	OKAY	1.2227
A11	IDH3G	1.0023	(0.94, 1.07)	OKAY	1.0023
A12	ACO1	1.2026	(1.11, 1.29)	OKAY	1.2026
B1	ACO2	0.914	(0.86, 0.97)	OKAY	-1.0941
B2	SDHA	0.7583	(0.71, 0.81)	OKAY	-1.3188
B3	SDHB	1.1257	(1.06, 1.20)	OKAY	1.1257
B4	ELOVL5	1.0801	(1.04, 1.12)	OKAY	1.0801
B5	ACOT1	1.0399	(0.97, 1.11)	OKAY	1.0399
B6	ELOVL1	1.1637	(1.06, 1.27)	OKAY	1.1637
B7	ELOVL3	1.1467	(1.03, 1.27)	B	1.1467
B8	ELOVL4	1.9534	(1.79, 2.11)	OKAY	1.9534
B9	ELOVL6	1.5785	(1.54, 1.62)	OKAY	1.5785
B10	ELOVL7	1.9403	(1.78, 2.10)	A	1.9403
B11	ACLY	1.3521	(1.31, 1.40)	OKAY	1.3521
B12	ACACA	1.0014	(0.90, 1.10)	OKAY	1.0014
C1	HMGCR	1.1344	(1.08, 1.19)	OKAY	1.1344
C2	LPIN	1.466	(1.29, 1.64)	OKAY	1.466
C3	FASN	0.3788	(0.29, 0.47)	OKAY	-2.6396
C4	SCD	0.332	(0.32, 0.34)	OKAY	-3.0121
C5	HCS1	1.9319	(1.83, 2.04)	OKAY	1.9319
C6	HCS2	0.5156	(0.47, 0.57)	OKAY	-1.9396
C7	ACTB	1.0922	(1.01, 1.17)	OKAY	1.0922
C8	GAPDH	1.0212	(1.00, 1.04)	OKAY	1.0212
C9	GNS	1.332	(1.29, 1.38)	OKAY	1.332
C10	GFPT1	1.3493	(1.28, 1.42)	OKAY	1.3493
C11	UGDH	1.4545	(1.40, 1.51)	OKAY	1.4545
C12	FH	1.0829	(1.05, 1.11)	OKAY	1.0829
D1	GLUD1	1.0061	(1.00, 1.01)	OKAY	1.0061
D2	GLUD2	1.1698	(1.15, 1.19)	OKAY	1.1698
D3	GLS	0.9269	(0.89, 0.96)	OKAY	-1.0788
D4	GLS2	0.8775	(0.82, 0.94)	OKAY	-1.1396
D5	ACTB	1.1303	(1.12, 1.14)	OKAY	1.1303
D6	GAPDH	0.953	(0.92, 0.98)	OKAY	-1.0493
D7	PRPS1	1.4922	(1.47, 1.51)	OKAY	1.4922
D8	PRPS2	1.183	(1.12, 1.24)	OKAY	1.183
D9	G6PD	1.2178	(1.15, 1.29)	OKAY	1.2178
D10	PGLS	0.836	(0.78, 0.89)	OKAY	-1.1961
D11	PGD	1.2016	(1.14, 1.26)	OKAY	1.2016
D12	RBKS	1.2803	(1.16, 1.40)	OKAY	1.2803

E1	RGN	1.3329	(1.22, 1.44)	C	1.3329
E2	MCATa	1.1351	(1.11, 1.16)	OKAY	1.1351
E3	MCATb	1.326	(1.21, 1.44)	OKAY	1.326
E4	ACACB	1.0898	(1.00, 1.18)	OKAY	1.0898
E5	OXSM	0.9587	(0.87, 1.04)	OKAY	-1.0431
E6	OLAH	3.0405	(2.92, 3.16)	OKAY	3.0405
E7	ACAA2	1.0987	(0.99, 1.20)	OKAY	1.0987
E8	ACOT2	0.9204	(0.91, 0.94)	A	-1.0865
E9	ACOT7	1.3237	(1.02, 1.63)	B	1.3237
E10	ELOVL2	1.4038	(1.34, 1.46)	OKAY	1.4038
E11	ACTB	1.1039	(1.01, 1.20)	OKAY	1.1039
E12	GAPDH	0.8722	(0.81, 0.93)	OKAY	-1.1465
F1	PDHA1	1.1894	(1.02, 1.36)	OKAY	1.1894
F2	PDHA2	4.0942	(3.72, 4.47)	OKAY	4.0942
F3	PDHB	1.1421	(1.05, 1.23)	OKAY	1.1421
F4	PDK1	0.9349	(0.85, 1.02)	OKAY	-1.0696
F5	PDK2	1.016	(0.93, 1.11)	OKAY	1.016
F6	PDK3	0.6782	(0.62, 0.74)	OKAY	-1.4745
F7	PDK4	0.719	(0.65, 0.79)	OKAY	-1.3908
F8	SDHC	0.877	(0.79, 0.96)	OKAY	-1.1402
F9	SDHD	1.0713	(1.00, 1.14)	OKAY	1.0713
F10	ACAA1	1.2875	(1.18, 1.40)	OKAY	1.2875
F11	ACAA2	0.8794	(0.81, 0.95)	OKAY	-1.1371
F12	ACAD10	0.7045	(0.65, 0.76)	OKAY	-1.4195
G01	ACAD11	1.4892	(1.36, 1.61)	OKAY	1.4892
G02	ACAD9	1.0386	(0.95, 1.13)	OKAY	1.0386
G03	ACADL	3.3743	(3.09, 3.66)	OKAY	3.3743
G04	ACADM	0.6665	(0.61, 0.72)	OKAY	-1.5005
G05	ACADS	0.8613	(0.79, 0.93)	A	-1.161
G06	ACADSB	0.6573	(0.60, 0.71)	A	-1.5214
G07	ACADVL	1.0752	(0.98, 1.17)	OKAY	1.0752
G08	ACAT1	1.7346	(1.59, 1.88)	OKAY	1.7346
G09	ACAT2	0.6852	(0.63, 0.74)	OKAY	-1.4594
G10	ACOT1	1.3329	(1.22, 1.44)	C	1.3329
G11	ACOT12	1.3329	(1.22, 1.44)	C	1.3329
G12	ACOT2	0.8673	(0.79, 0.94)	OKAY	-1.153
H01	ACOT6	1.2523	(1.15, 1.36)	OKAY	1.2523
H02	ACOT7	0.969	(0.89, 1.05)	OKAY	-1.032
H03	ACOT8	0.4489	(0.41, 0.49)	OKAY	-2.2275
H04	ACOT9	1.3704	(1.26, 1.49)	OKAY	1.3704
H05	ACOX1	0.7871	(0.72, 0.85)	OKAY	-1.2705
H06	ACOX2	0.5086	(0.47, 0.55)	OKAY	-1.9662
H07	ACOX3	0.8979	(0.82, 0.97)	OKAY	-1.1137
H08	ACSBG1	1.3515	(1.24, 1.47)	OKAY	1.3515
H09	ACSBG2	0.7094	(0.65, 0.77)	A	-1.4097
H10	ACSL1	1.4996	(1.37, 1.63)	OKAY	1.4996
H11	ACSL3	0.5883	(0.54, 0.64)	OKAY	-1.6999
H12	ACSL4	1.1054	(1.01, 1.20)	OKAY	1.1054
I1	ACSL5	2.1804	(2.00, 2.36)	OKAY	2.1804
I2	ACSL6	0.9231	(0.85, 1.00)	B	-1.0833
I3	ACSM2A	1.3329	(1.22, 1.44)	C	1.3329
I4	ACSM3	0.8494	(0.78, 0.92)	OKAY	-1.1772

I5	ACSM4	1.3329	(1.22, 1.44)	C	1.3329
I6	ACSM5	1.3329	(1.22, 1.44)	C	1.3329
I7	ALDH2	1.0314	(0.94, 1.12)	B	1.0314
I8	BDH1	1.3515	(1.24, 1.47)	OKAY	1.3515
I9	BDH2	0.6852	(0.63, 0.74)	OKAY	-1.4594
I10	CPT1A	1.2965	(1.19, 1.41)	OKAY	1.2965
I11	CPT1B	0.9623	(0.88, 1.04)	OKAY	-1.0392
I12	CPT1C	0.9041	(0.83, 0.98)	OKAY	-1.1061
J1	CPT2	1.5205	(1.39, 1.65)	OKAY	1.5205
J2	CRAT	1.2181	(1.12, 1.32)	OKAY	1.2181
J3	CROT	0.5193	(0.48, 0.56)	OKAY	-1.9257
J4	DECR1	1.0243	(0.94, 1.11)	OKAY	1.0243
J5	DECR2	1.3704	(1.26, 1.49)	OKAY	1.3704
J6	ECHS1	0.6948	(0.64, 0.75)	OKAY	-1.4394
J7	EHHADH	0.8205	(0.75, 0.89)	OKAY	-1.2188
J8	FABP1	1.3329	(1.22, 1.44)	C	1.3329
J9	FABP2	1.2965	(1.19, 1.41)	OKAY	1.2965
J10	FABP3	1.1766	(1.08, 1.28)	OKAY	1.1766
J11	FABP4	0.6852	(0.63, 0.74)	OKAY	-1.4594
J12	FABP5	1.2523	(1.15, 1.36)	OKAY	1.2523
K1	FABP6	3.903	(3.57, 4.23)	A	3.903
K2	GCDH	1.1684	(1.07, 1.27)	OKAY	1.1684
K3	GK	0.4981	(0.46, 0.54)	OKAY	-2.0075
K4	GK2	1.3329	(1.22, 1.44)	C	1.3329
K5	GPD1	1.2965	(1.19, 1.41)	OKAY	1.2965
K6	GPD2	0.6349	(0.58, 0.69)	OKAY	-1.5751
K7	HADHA	0.936	(0.86, 1.01)	OKAY	-1.0684
K8	HMGCL	1.0678	(0.98, 1.16)	OKAY	1.0678
K9	HMGCS1	1.0386	(0.95, 1.13)	OKAY	1.0386
K10	HMGCS2	1.1286	(1.03, 1.22)	B	1.1286
K11	LIPE	0.9557	(0.88, 1.04)	B	-1.0464
K12	LPL	1.3329	(1.22, 1.44)	C	1.3329
L1	MCEE	2.2417	(2.05, 2.43)	OKAY	2.2417
L2	MUT	1.1054	(1.01, 1.20)	OKAY	1.1054
L3	OXCT2	0.5413	(0.50, 0.59)	OKAY	-1.8473
L4	ECI2	0.7709	(0.71, 0.84)	OKAY	-1.2972
L5	PECR	1.3237	(1.21, 1.43)	OKAY	1.3237
L6	PPA1	0.9104	(0.83, 0.99)	OKAY	-1.0984
L7	PRKAA1	1.2965	(1.19, 1.41)	OKAY	1.2965
L8	PRKAA2	1.5851	(1.45, 1.72)	OKAY	1.5851
L9	PRKAB1	0.7603	(0.70, 0.82)	OKAY	-1.3153
L10	PRKAB2	1.4385	(1.32, 1.56)	OKAY	1.4385
L11	PRKACA	1.0172	(0.93, 1.10)	OKAY	1.0172
L12	PRKACB	0.6175	(0.57, 0.67)	OKAY	-1.6194
M1	PRKAG1	1.641	(1.50, 1.78)	OKAY	1.641
M2	PRKAG2	1.3237	(1.21, 1.43)	OKAY	1.3237
M3	PRKAG3	0.9894	(0.91, 1.07)	B	-1.0107
M4	SLC27A1	0.832	(0.76, 0.90)	A	-1.202
M5	SLC27A2	1.4385	(1.32, 1.56)	OKAY	1.4385
M6	SLC27A3	0.5265	(0.48, 0.57)	OKAY	-1.8992
M7	SLC27A4	1.2965	(1.19, 1.41)	OKAY	1.2965
M8	SLC27A5	1.6184	(1.48, 1.75)	OKAY	1.6184

M9	SLC27A6	0.3045	(0.28, 0.33)	OKAY	-3.2839
Comments:					
A: This gene's average threshold cycle is relatively high (> 30) in either the control or the test sample, and is reasonably low in the other sample (< 30).					
These data mean that the gene's expression is relatively low in one sample and reasonably detected in the other sample suggesting that the actual fold-change value is at least as large as the calculated and reported fold-change result.					
This fold-change result may also have greater variations if p value > 0.05; therefore, it is important to have a sufficient number of biological replicates to validate the result for this gene.					
B: This gene's average threshold cycle is relatively high (> 30), meaning that its relative expression level is low, in both control and test samples, and the p-value for the fold-change is either unavailable or relatively high (p > 0.05).					
This fold-change result may also have greater variations; therefore, it is important to have a sufficient number of biological replicates to validate the result for this gene.					
C: This gene's average threshold cycle is either not determined or greater than the defined cut-off value (default 35), in both samples meaning that its expression was undetected, making this fold-change result erroneous and un-interpretable.					
Fold Change & Fold Regulation:					
Fold-Change ($2^{(-\Delta\Delta Ct)}$) is the normalized gene expression ($2^{(-\Delta Ct)}$) in the Test Sample divided the normalized gene expression ($2^{(-\Delta Ct)}$) in the Control					
Fold-Regulation represents fold-change results in a biologically meaningful way. Fold-change values greater than one indicate a positive- or an up-regulation, and the fold-regulation is equal to the fold-change.					
Fold-change values less than one indicate a negative or down-regulation, and the fold-regulation is the negative inverse of the fold-change.					
Fold-change and fold-regulation values greater than 2 are indicated in red; fold-change values less than 0.5 and fold-regulation values less than -2 are indicated in blue.					

Supplementary Procedures

Oil Red-O Staining

Cells were grown on coverslips placed in a six-well plate until 80% confluent. Cell culture medium were aspirated and cells were washed with PBS, and then fixed by adding 2mL of 10% formalin for 30 minutes, followed by 60% isopropanol for 5 minutes. Oil Red O stock solution was then diluted and filtered according to manufacturer's protocol (Cayman Chemicals), and finally added to stain the cells for 5 minutes. Cells were washed, dried and coverslips were mounted on slides using prolong gold anti-fade DAPI (Invitrogen). Slides were imaged using Olympus microscope.

Oxygen Consumption

The oxygen consumption rate (OCR) was measured using a Seahorse Bioscience XF24 Extracellular Flux Analyzer according to manufacturer's protocol. Briefly, cells were seeded in triplicates at equal densities (25,000 cells per well) into XF24 tissue culture plates. For nutrient stressed conditions, cell media was changed 12 hr after cell seeding into high glucose/low glutamine or low glucose/high glutamine. Oxygen consumption was measured under basal conditions (DMSO), oligomycin and mitochondrial uncoupler trifluoromethoxy carbonyl cyanide phenyl hydrazone (FCCP) (2 mM) using the mito-stress kit (Seahorse Bioscience). Oxygen consumption values were normalized to cell number.

siRNA, Adenovirus and Mutagenesis

siRNAs targeting SRC-2, SREBP-1, SCD, mTOR and GFP were obtained from Invitrogen and Dharmacon and Lipofectamine 2000 (Invitrogen, CA) was used for transfection. SRC-2 siRNAs used are: siSRC-2 (#1: HSS116116; #2: HSS116117) from Invitrogen; and siSRC-2 (L-

020159SREBF1 (L-006891); siSREBF1 (L-006891); siSCD (L-005061-00-0005); siMTOR (D-003008-05, 06, 07); non-targeting siRNA (D-001810) from Dharmacon; and control GFP-siRNA (12935-145) from Invitrogen. SRC-2 mutants were generated using site-directed mutagenesis (Stratagene). Adenovirus expressing full-length human SRC-2, SRC-2 mutants and GFP were cloned in pAdeno-X (Clontech) plasmid and virus was amplified and purified at Gene Vector Core Laboratory, BCM. Purified virus was then used to infect human prostate cancer cells. Adenovirus expressing FASN (Catalog #: SL100773) and Zip1 (Catalog #: SL182025) were obtained from Signagen.

Measurement of Glucose, Glutamine and ATP levels

Glucose and glutamine consumption were measured in LNCaP, C4-2 and PC-3 cells transfected with siRNAs targeting GFP or SRC-2, using Biovision Kits (Cat# K606-100 and K629-100), according to manufacturer's instructions. Briefly, cells were starved overnight in low glucose/low glutamine medium (0.2mM L-Glutamine and 5mM D-Glucose) followed by incubation in complete media containing 11mM D-Glucose and 2mM-L-Glutamine. Cells were harvested at each hour time points for 6 hours, followed by colorimetric estimation of cell lysates and spent media. Data collected was then background corrected from time (t=0) and the amount of metabolite consumed was calculated per hour normalized to total protein. ATP levels in the cell were measured using StayBrite Highly Stable ATP assay (Biovisoin). Briefly, cells lysates were mixed in reaction buffer, and luminescent readings were acquired using Berthold 96 well plate reader. ATP levels were calculated based on a standard curve of known ATP concentrations and data generated was normalized to total protein concentration.

Luciferase Assay

Luciferase promoter constructs were obtained from following sources: FASN-Addgene, SCD-Switchgear genomics and ZIP1- Peter Makhov (Fox Chase Cancer Center). FASN-luc (25ng or

75ng), SCD-luc (100ng or 500ng) and ZIP1-luc (100ng or 500ng) promoter constructs were transfected into HeLa cells or PC-3 cells, respectively seeded in twenty-four well plates at the indicated concentrations along with SREBP-1 (20ng/well) and SRC-2 (50ng/well). Control lanes were transfected with empty vector and the total amount of DNA in each well were normalized by adding blank-plasmids. Cells were harvested two days after transfection and luciferase assay performed using a Luciferase Reporter Assay (Promega) and a Berthold 96 well plate reader. Luciferase values were normalized to the total protein level.

Gene Expression Analyses

Total mRNA was isolated from prostate cancer cells, tissues and tumors using the RNeasy Kit (QIAGEN). Reverse transcription was carried out using Superscript VILO cDNA synthesis kit (Invitrogen, CA) according to the manufacturer's instructions. For gene expression analysis, qPCR was performed using the Taqman system (Roche) with sequence-specific primers and the Universal Probe Library (Roche). Actin was used as an internal control. Melting curve analysis was performed to ensure that a single PCR product expected was produced in a given well. We used 3 biological replicates for each treatment group. Data was analyzed using the comparative Ct method ($\Delta\Delta C_t$). In addition, a human fatty acid metabolism PCR array Cat#PAHS-007Z (SA Biosciences, CA) was used to measure 84 key genes involved in the regulation and enzymatic pathways of fatty acid metabolism using SYBER green (QIAGEN), according to the manufacturer's instructions. Data obtained was analyzed using RT² Profiler™ PCR Array Data Analysis software (SA Biosciences, CA). Primer sequences are available on request.

Cell growth and clonogenic survival assays

Cells were seeded in 96-well plates in complete medium, and after the cells attached to the bottom surface they were incubated in nutrient-stressed medium. The cell growth was

measured using Cellglo kit (Promega) according to manufacturer's instructions. For the clonogenic survival assays, 200 cells per well were plated onto a 6-well plate, and were incubated in nutrient-stressed medium for 14 days, and stained with crystal violet. For the rescue experiment respective adenovirus were added in the medium. The medium was changed every two days.

Soft-agar colony formation assay

The assay was performed with C4-2 and PC-3 stable cells using a cell transformation detection assay kit (Millipore), according to manufacturer's protocol. Briefly, 1500cells/well were mixed with 0.4% top agar solution and layered on top of 0.8% agar base layer, and finally covered with complete growth medium. The colonies formed were detected by addition of cell stain solution after 10 days and were imaged by UVP-Biospectrum.

Cycloheximide protein stability assays

SRC-2 protein stability was studied by cycloheximide treatment experiments in C4-2 cells for different time points as described previously (3). C4-2 cells were cultured in low glutamine (0.2mM) or high glutamine (2.0mM) followed by treatment with cycloheximide (0.5mM). For Torin treatment, C4-2 cells cultured in high glutamine were either treated with DMSO (vehicle-control) or Torin (250nM) prior to cyclohexamide treatments. Cells were lysed followed by Western immunoblotting.

Chromatin immunoprecipitation (ChIP)

The following antibodies were used for ChIP: SRC-2 (Bethyl Laboratories), SREBP-1 (Santacruz), rabbit IgG, and mouse IgG. ChIP assays were performed according to an EZ ChIP kit (Millipore) with some modification (4). Briefly, C4-2 stable cells were grown in 15 cm dishes until 80% confluent. For glutamine stimulation, cells were glutamine-deprived overnight by

incubating in low glutamine medium (0.2mM L-Glutamine and 11mM D-Glucose), followed by 4 hours pre-treatment with or without Torin (250nM), a mTORC1 selective inhibitor, and with/without high glutamine (2mM L-glutamine and 11mM D-glucose) treatment for one hour, before crosslinking in 1% formaldehyde and quenching with glycine. Chromatin was sheared by sonication using a Sonifier, precleared with control IgG antibodies and agarose beads (Millipore), and then immunoprecipitated with IgG (control), SRC-2 and SREBP-1 antibodies. DNA fragments were eluted from beads followed by reverse-crosslinking and purified DNA was used in qPCR reactions using SYBR green to determine the promoter occupancy.

Androgen and SRC-2 response gene signatures

The androgen response gene signatures were derived as previously described (5). The LNCaP siAR gene signature was derived after treating LNCaP cells in full media with siAR (Invitrogen) for 72 hours. The siSRC2 gene signature was derived after treating LNCaP cells in full media with siSRC2 (Invitrogen) for 48 hours. Gene expression profiling was carried out utilizing the Affymetrix Human Exon 1.0 ST Array platform at the Genomic and RNA Profiling Core (G.A.R.P.) at Baylor College of Medicine. Gene expression differences were inferred utilizing the t-test ($p < 0.05$) and imposing a fold change exceeding 4/3x, using the R statistical system.

Experimental lung metastasis

PC-3 stable cells expressing control shNT, SRC-2 sh18, and sh19 were trypsinized, washed with PBS, and finally resuspended in PBS (5×10^6 cells/mL). Two hundred μ l of the cell suspension (1×10^6 cells/mL) was injected via tail-vein into each Nude male mouse (Harlan Laboratories) at the age of 6 to 7 weeks ($n=7$). Mice were sacrificed 5 weeks after injection and lungs were perfused with PBS and excised. Part of the lung was fixed in 4% paraformaldehyde, embedded in paraffin, and sectioned at a thickness of 4 μ m for histological examination by H&E staining.

Prostate cancer orthotopic mouse model

PC-3 stable cells expressing control shNT and SRC-2-sh19 (GFP-labeled) were injected orthotopically into the prostates of 8- to 10-week-old SCID mice ($n=5$), using 1×10^6 cells in a volume of 20 μ L (6). Mice were sacrificed at 10 weeks after injection, and the primary tumor foci and metastatic lesions were analyzed by GFP-imaging. The primary tumor volume was calculated using $[ab^2 \times 0.5, \text{ where } a > b]$ using slide calipers and the number of GFP-positive metastatic lesions were also counted.

Cell culture treatment conditions, protein isolation and Western blotting

For, siRNA treatments cells were lysed 72 hours post-transfection. Stable cells were grown till 80% confluency before protein was extracted. During nutritional stress conditions, stable cells were cultured in complete media till 80% confluency, followed by an overnight starvation in low glucose/low glutamine medium (0.2mM L-Glutamine and 5mM D-Glucose). Cells were then switched to high glucose (11mM)/ low glutamine (0.2mM) medium, or high glutamine (2mM)/low glucose (5mM) medium, as indicated in the figures, for 24 hours before cells were lysed. For kinase inhibitor treatments, cells were incubated in indicated medium along with inhibitors for 12 hours before cells were harvested and lysed. Western blot was performed as described previously (7). Briefly, cells were lysed using NP-40 lysis buffer (Invitrogen, CA) along with protease and phosphatase inhibitor cocktail (Millipore). Total protein was estimated using BCA-protein estimation kit (Pierce) and approximately 40 μ g of proteins were separated by 4-12% Bis-Tris gels (Invitrogen) and electroblotted onto nitrocellulose membranes using the iBlot system (Invitrogen). Blots were blocked for 2 hour at room temperature or overnight at 4° C in 1 X TBS buffer (Biorad, CA) supplemented with 0.1% Tween-20 (Sigma, MO) supplemented with 5% bovine serum albumin (BSA) or 5% non-fat dry milk (Biorad, CA). Blots were incubated overnight at 4°C with primary antibody diluted into TBST containing 1% BSA or 5% non-fat dry

milk. Blots were subsequently washed three times for 10 mins in TBST and incubated with secondary antibody coupled to horseradish peroxidase (Promega). Blots were washed as previously described, reacted with ECL reagents (Thermo Scientific) and detected by chemiluminescence (UVP Biospectrum).

Immunoprecipitations

C4-2 cells were cultured in five 100mm dishes until 80% confluency, followed by infection with Adv. GFP (one plate) or Adv. SRC-2 (expressing HA-tagged SRC-2) in four plates. Twenty four hours post-infection media was changed and cells were incubated overnight in low glutamine medium (0.2mM L-Glutamine and 11mM D-Glucose, and 10% dialyzed-FBS). C4-2 cells expressing Adv. SRC-2 were pre-treated for 4 hours with either DMSO or Torin (250nM), a mTORC1 selective inhibitor and then stimulated with different concentrations of L-Glutamine (0.2mM, 2mM, and 4mM) supplemented with 11mM D-glucose and 10% dialyzed serum as indicated in the figure for one hour. Cells were lysed in NP-40 lysis buffer (Invitrogen) supplemented with protease and phosphatase inhibitor cocktail (Millipore) and precleared with control Protein A/G Agarose beads (Pierce). Five hundred micrograms of protein were then used for pulldown assays using monoclonal anti-HA-agarose antibody beads (Sigma) overnight. The beads were then captured, washed and immunoprecipitated proteins were eluted and subjected to western blotting, along with 2% input sample.

Immunohistochemistry

Immunohistochemistry was performed as described previously (Han, Hawkins, et al, 2012). Mouse monoclonal anti-human Ki-67 antibody MIB-1 (Dako) was used to stain the lungs sections followed by anti-mouse Alexa-594 secondary antibody (Molecular Probes).

RNA-seq Data Analysis

The RNA-Seq data was reported earlier (8) consisting of a cohort comprised of 132 prostate tissues sequenced at MCTP (Michigan Center for Translational Pathology) at University of Michigan. Sequencing data were aligned using TopHat 2.0.8 against the Ensembl 69 GRCh37 human genome build and FPKM was calculated across genes in Ensembl 69 using Cufflinks 2.0.2. Graphs were created using a variety of custom R and python scripts.

Supplemental References

1. Sreekumar, A., Poisson, L.M., Rajendiran, T.M., Khan, A.P., Cao, Q., Yu, J., Laxman, B., Mehra, R., Lonigro, R.J., Li, Y. et al. 2009. Metabolomic profiles delineate potential role for sarcosine in prostate cancer progression. *Nature* **457**:910-914.
2. Putluri, N., Shojaie, A., Vasu, V.T., Nalluri, S., Vareed, S.K., Putluri, V., Vivekanandan-Giri, A., Byun, J., Pennathur, S., Sana, T.R. et al. 2011. Metabolomic profiling reveals a role for androgen in activating amino acid metabolism and methylation in prostate cancer cells. *PLoS One* **6**:e21417.
3. Li, C., Ao, J., Fu, J., Lee, D.F., Xu, J., Lonard, D., and O'Malley, B.W. 2011. Tumor-suppressor role for the SPOP ubiquitin ligase in signal-dependent proteolysis of the oncogenic co-activator SRC-3/AIB1. *Oncogene* **30**:4350-4364.
4. Foulds, C.E., Feng, Q., Ding, C., Bailey, S., Hunsaker, T.L., Malovannaya, A., Hamilton, R.A., Gates, L.A., Zhang, Z., Li, C. et al. 2013. Proteomic analysis of coregulators bound to ERalpha on DNA and nucleosomes reveals coregulator dynamics. *Mol. Cell* **51**:185-199.

5. Wang, Q., Li, W., Liu, X.S., Carroll, J.S., Janne, O.A., Keeton, E.K., Chinnaiyan, A.M., Pienta, K.J., and Brown, M. 2007. A hierarchical network of transcription factors governs androgen receptor-dependent prostate cancer growth. *Mol. Cell* **27**:380-392.
6. Yu, W., Feng, S., Dakhova, O., Creighton, C.J., Cai, Y., Wang, J., Li, R., Frolov, A., Ayala, G., and Ittmann, M. 2011. FGFR-4 Arg(3)(8)(8) enhances prostate cancer progression via extracellular signal-related kinase and serum response factor signaling. *Clin. Cancer Res.* **17**:4355-4366.
7. York, B., Reineke, E.L., Sagen, J.V., Nikolai, B.C., Zhou, S., Louet, J.F., Chopra, A.R., Chen, X., Reed, G., Noebels, J. et al. 2012. Ablation of steroid receptor coactivator-3 resembles the human CACT metabolic myopathy. *Cell. Metab.* **15**:752-763.
8. Kaushik, A.K., Vareed, S.K., Basu, S., Putluri, V., Putluri, N., Panzitt, K., Brennan, C.A., Chinnaiyan, A.M., Vergara, I.A., Erho, N. et al. 2014. Metabolomic profiling identifies biochemical pathways associated with castration-resistant prostate cancer. *J. Proteome Res.* **13**:1088-1100.

Unedited Gel Images

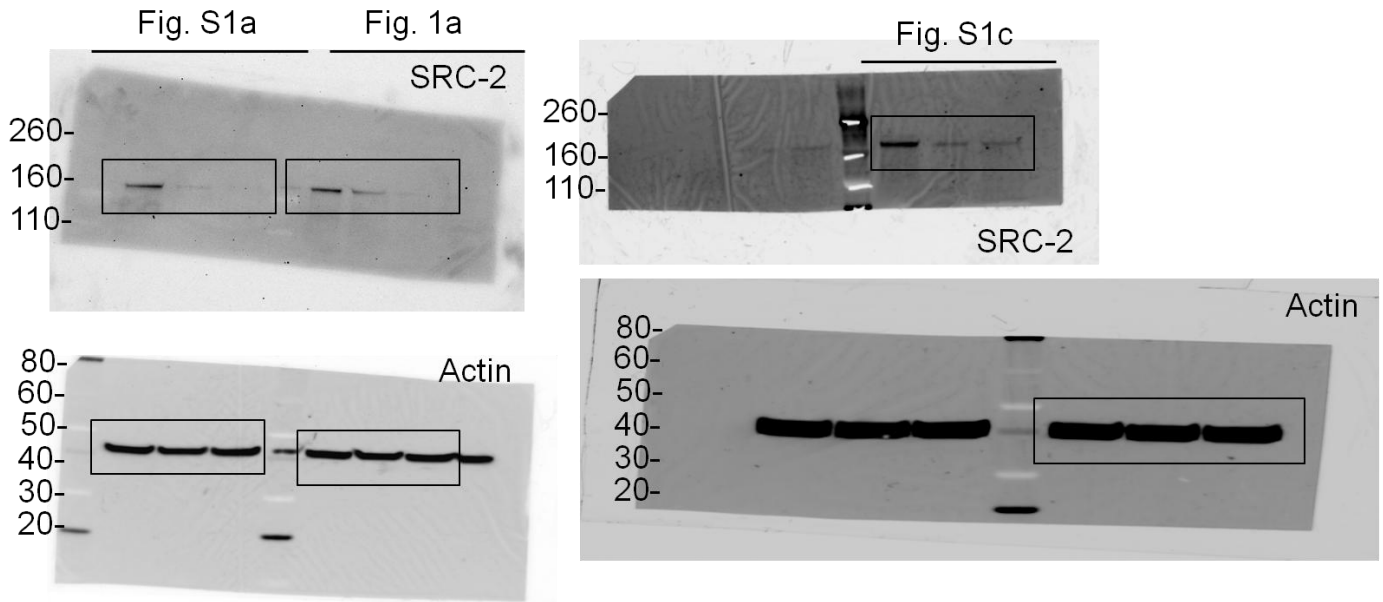


Fig. 2G

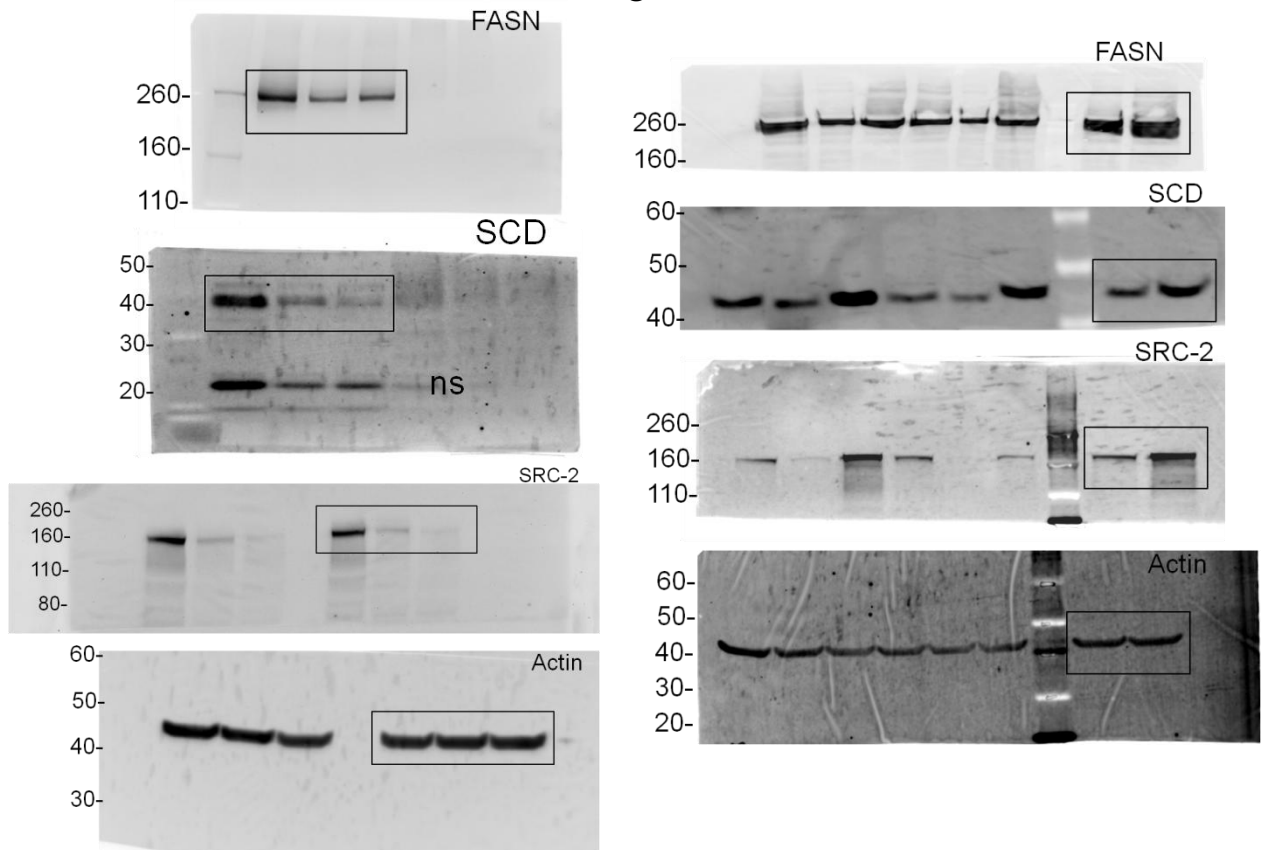


Fig. 3c

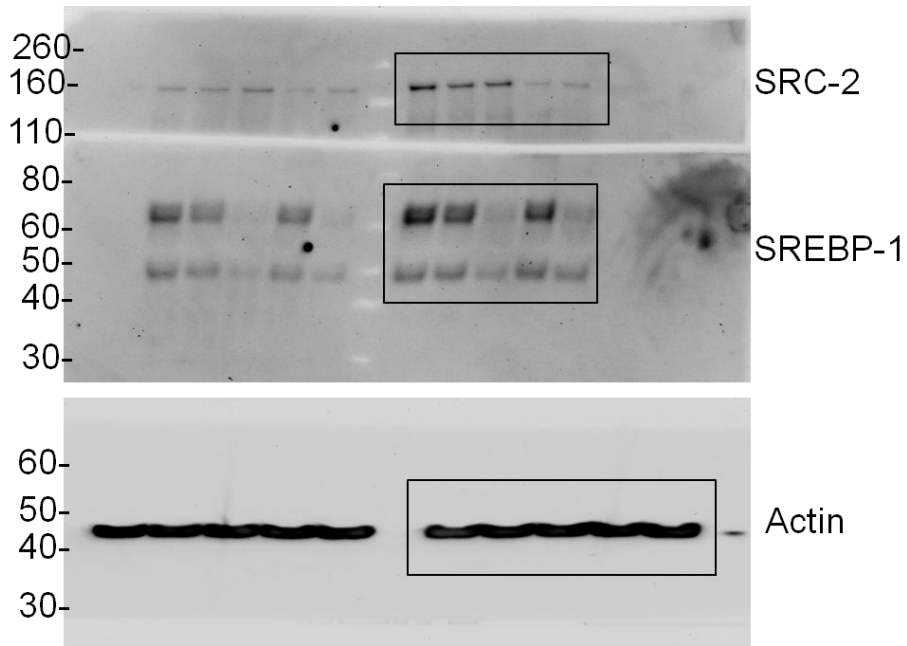


Fig. 5a

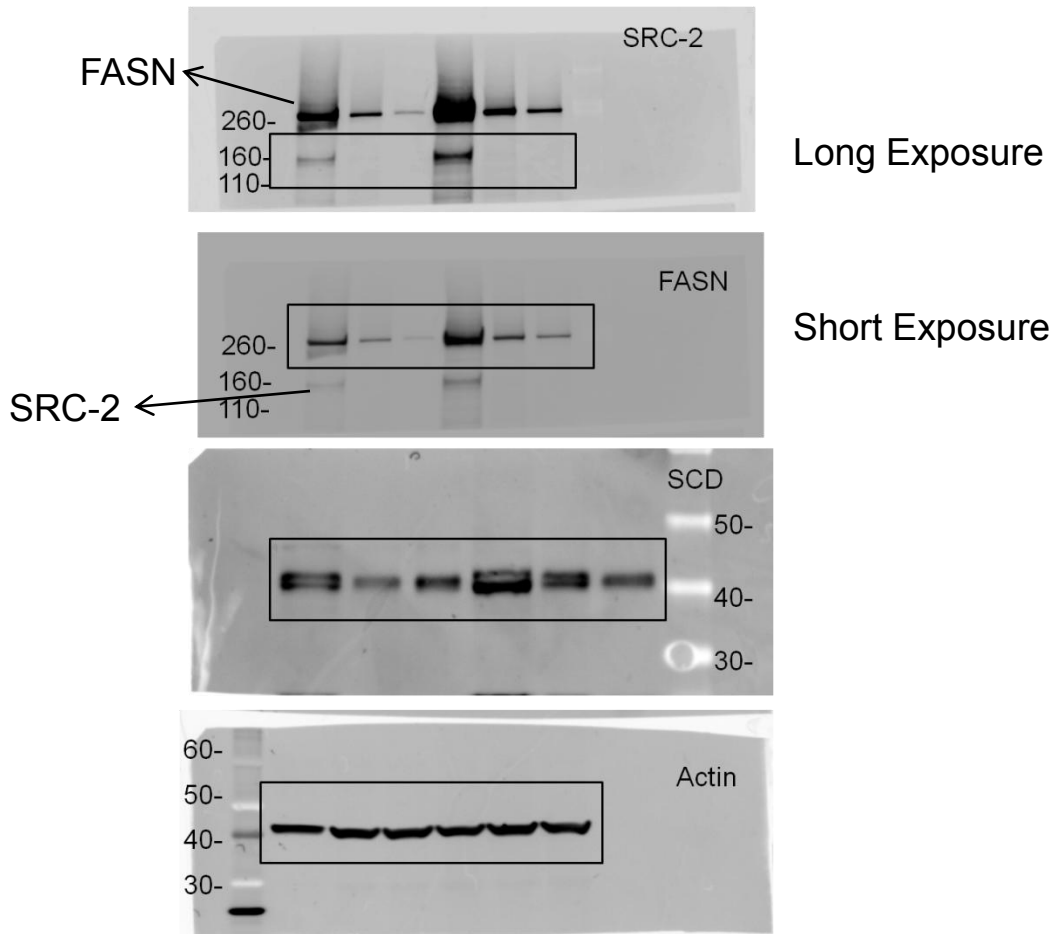


Fig. 5c

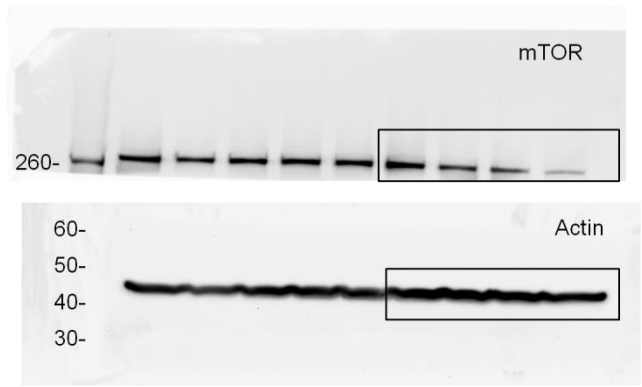


Fig. 5b

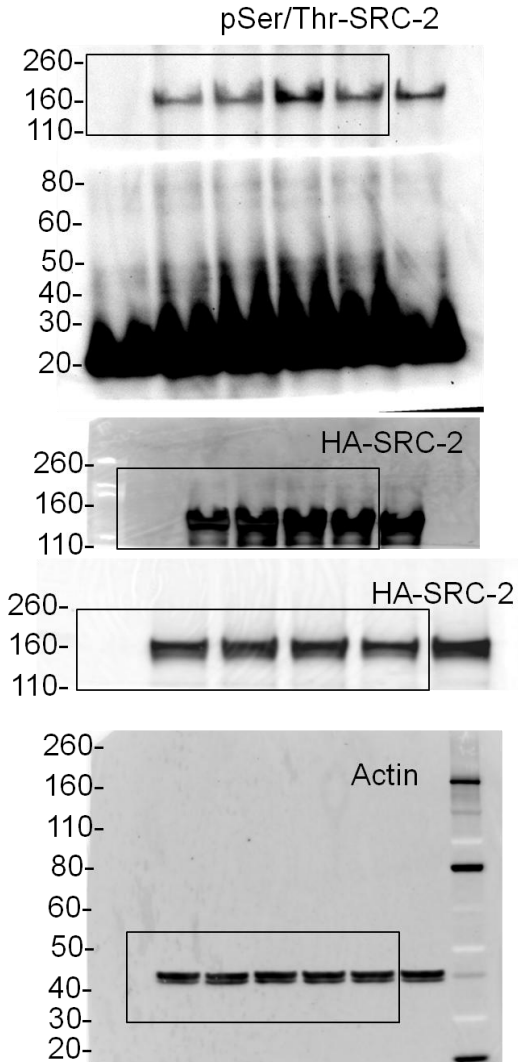


Fig. 5d

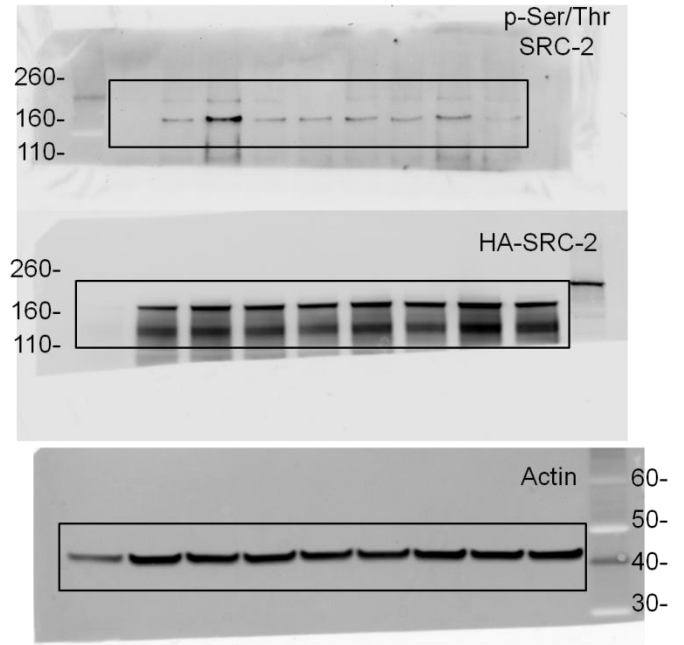


Fig. 5e

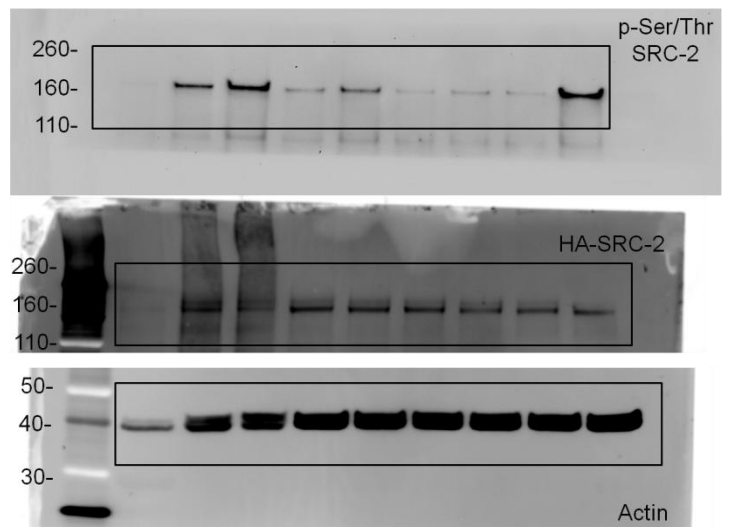


Fig. 6d

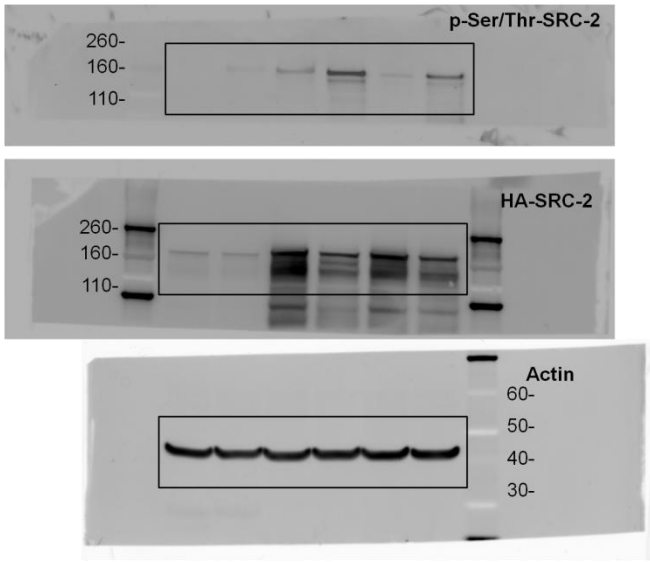


Fig. S7d

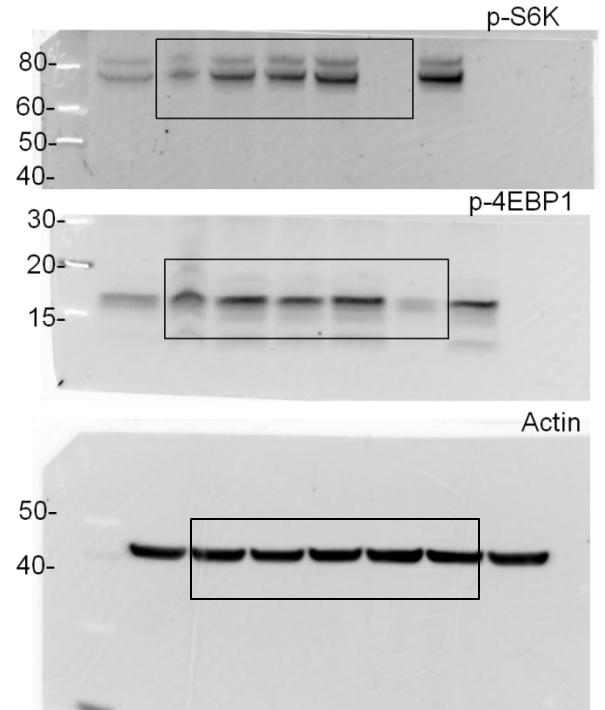


Fig. S7b

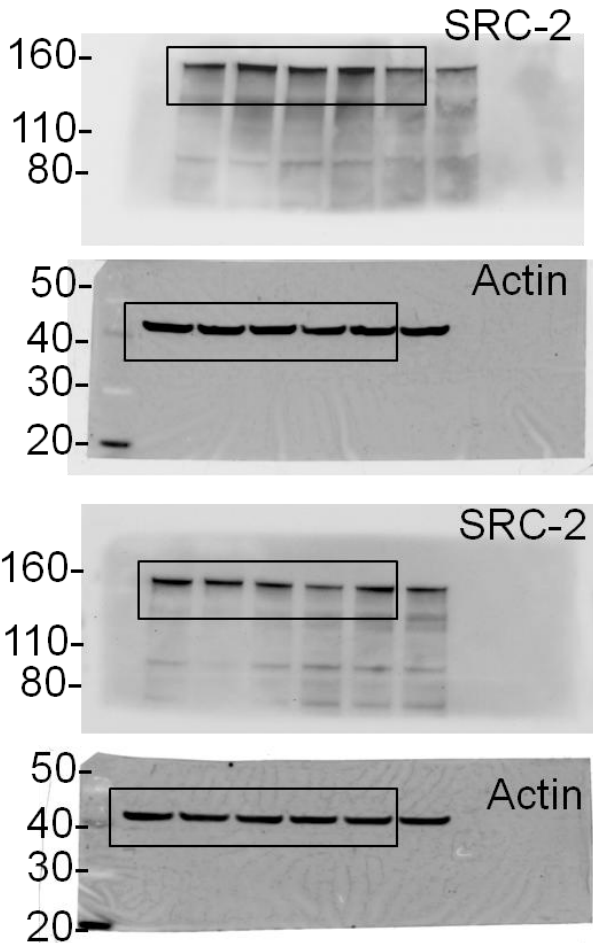


Fig. 8e

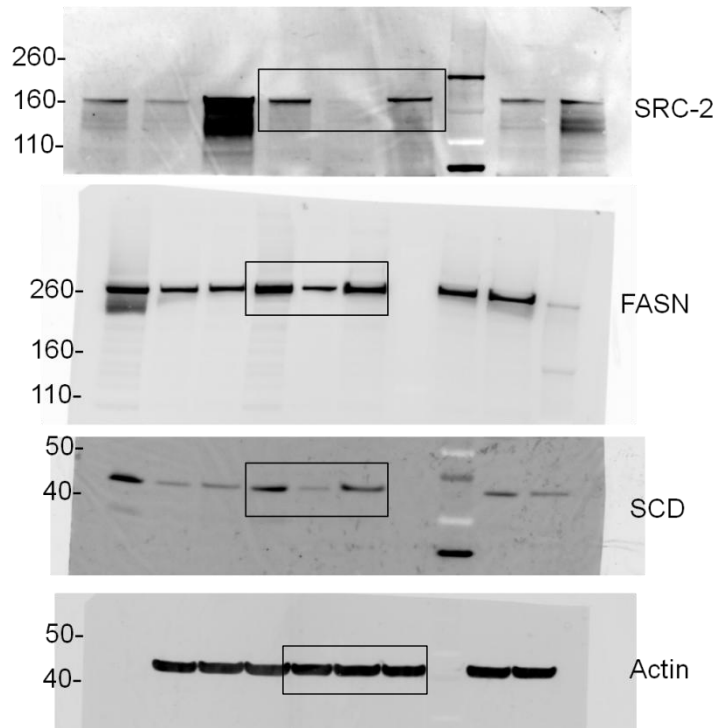
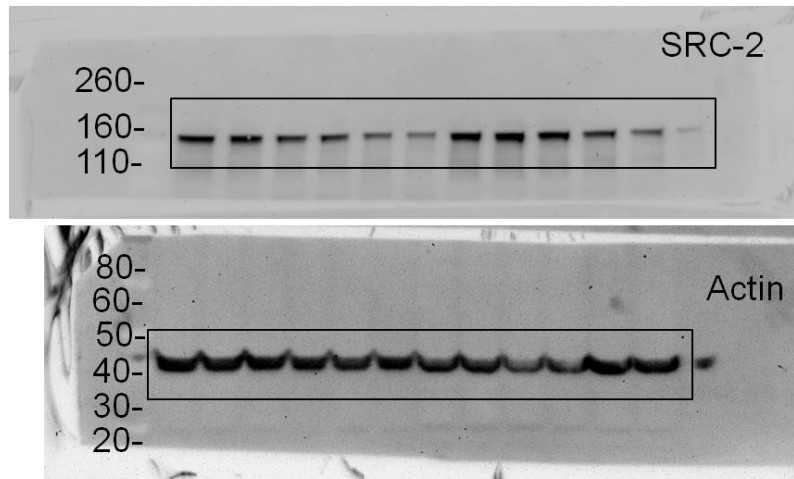


Fig. S8

A



B

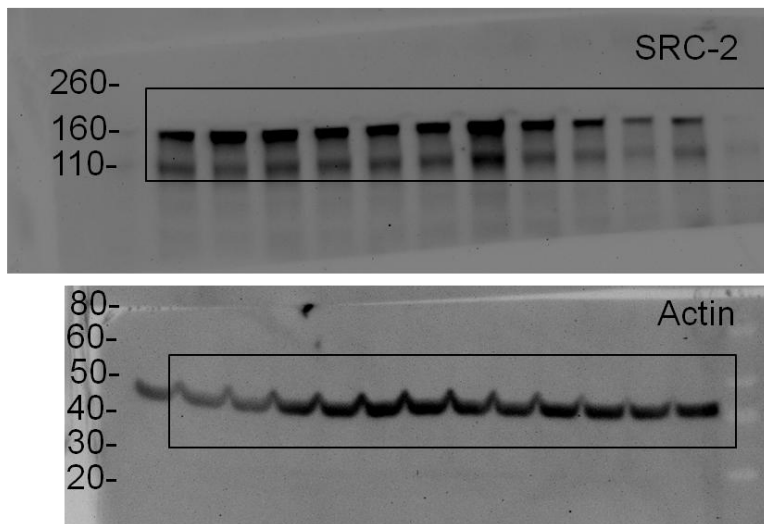


Fig. S11d

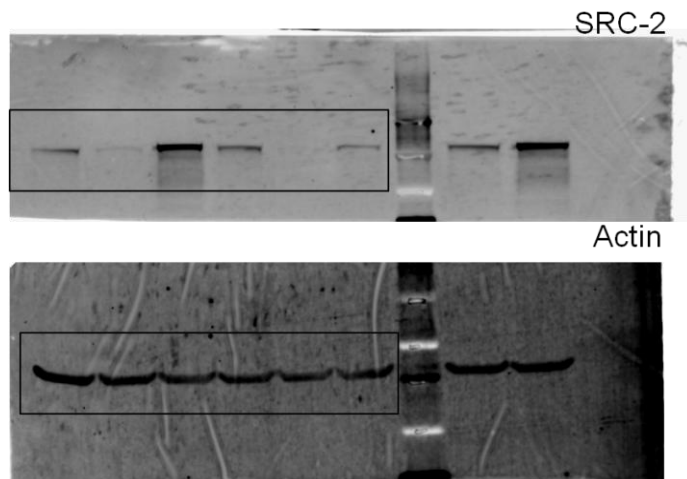


Fig. S12c

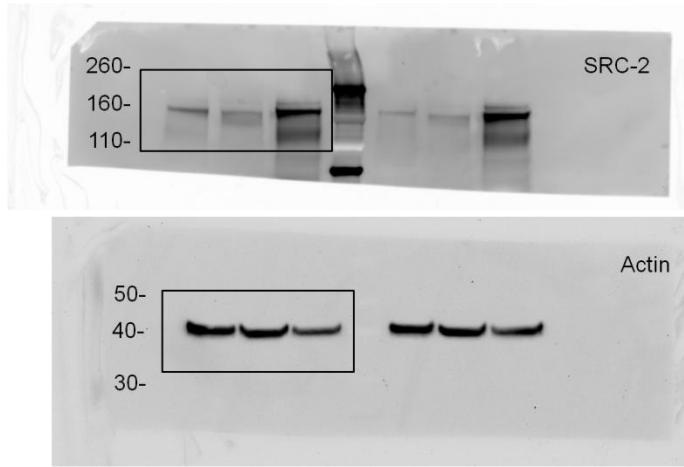


Fig. S12d

